Journal of Theoretical Biology 269 (2011) 16–30

Contents lists available at ScienceDirect

Journal of Theoretical Biology

journal homepage: www.elsevier.com/locate/yjtbi

The vertical distribution of phytoplankton in stratified water columns

Jarad P. Mellard [a,*], Kohei Yoshiyama [b], Elena Litchman [a,c], Christopher A. Klausmeier [a]

[a] W.K. Kellogg Biological Station and Department of Plant Biology, Michigan State University, Hickory Corners, MI 49060, USA
[b] Department of Chemical Oceanography, Ocean Research Institute, University of Tokyo, Tokyo, Japan
[c] Department of Zoology, Michigan State University, East Lansing, MI 48824, USA

ARTICLE INFO

Article history:
Received 17 December 2009
Received in revised form
23 September 2010
Accepted 28 September 2010

Keywords:
Spatial heterogeneity
Resource gradient
Resource competition
ESS
Algae

ABSTRACT

What determines the vertical distribution of phytoplankton in different aquatic environments remains an open question. To address this question, we develop a model to explore how phytoplankton respond through growth and movement to opposing resource gradients and different mixing conditions. We assume stratification creates a well-mixed surface layer on top of a poorly mixed deep layer and nutrients are supplied from multiple depth-dependent sources. Intraspecific competition leads to a unique strategic equilibrium for phytoplankton, which allows us to classify the distinct vertical distributions that can exist. Biomass can occur as a benthic layer (BL), a deep chlorophyll maximum (DCM), or in the mixed layer (ML), or as a combination of BL+ML or DCM+ML. The ML biomass can be limited by nutrients, light, or both. We predict how the vertical distribution, relative resource limitation, and biomass of phytoplankton will change across environmental gradients. We parameterized our model to represent potentially light and phosphorus limited freshwater lakes, but the model is applicable to a broad range of vertically stratified systems. Increasing nutrient input from the sediments or to the mixed layer increases light limitation, shifts phytoplankton towards the surface, and increases total biomass. Increasing background light attenuation increases light limitation, shifts the phytoplankton towards the surface, and generally decreases total biomass. Increasing mixed layer depth increases, decreases, or has no effect on light limitation and total biomass. Our model is able to replicate the diverse vertical distributions observed in nature and explain what underlying mechanisms drive these distributions.

1. Introduction

The aquatic environment of phytoplankton creates an opportune situation to study the feedbacks between resource gradients, behavioral movement, population dynamics, and passive dispersal. The major axis of spatial heterogeneity for phytoplankton is the vertical dimension. The vertical distribution of phytoplankton affects primary production as well as energy transfer to higher trophic levels (Leibold, 1990; Williamson et al., 1996; Lampert et al., 2003). Therefore, there is an immediate need to understand the fundamental principles that govern the vertical distribution of phytoplankton, ecologically important organisms that contribute roughly half of global net primary productivity (NPP) (Field et al., 1998) and continue to be affected by climate change (Hays et al., 2005).

A dizzying diversity of phytoplankton vertical distributions have been observed (see Fig. 1 for a few examples). Physical stratification breaks the water column into distinct strata resulting in non-uniform mixing, often with a well-mixed surface layer on top of a poorly mixed deep layer (Wetzel, 1975; Wüest et al., 2000). Phytoplankton may be found in high abundance in the mixed layer, in the deep layer, directly on the bottom, or in some combination of these layers. What determines their vertical distribution in stratified water columns? Light is in greatest supply at the top of the mixed layer and phytoplankton are hypothesized to exist there when there is adequate nutrient supply (Reynolds, 1984; Paerl, 1988). Frequently, phytoplankton form a peak in abundance known as a deep chlorophyll maximum, or DCM, in the deep layer. Low turbulence and sufficient light penetration have been hypothesized as necessary for a DCM to persist (Fee, 1976) and the light and nutrient gradients control the depth of the peak (Fee, 1976; Klausmeier and Litchman, 2001). Under low nutrient concentrations and if sufficient light penetrates to the bottom, algae may form a benthic layer on the sediments and access nutrients diffusing through the sediment pore water before it enters the water column (Sand-Jensen and Borum, 1991).

In a well-mixed water column, phytoplankton and nutrients are homogenized throughout the water column; however, a light gradient is inevitable. As a consequence, phytoplankton

* Corresponding author. Current address: Department of Ecology and Evolutionary Biology, University of Kansas, Lawrence KS, 66045, USA.
E-mail addresses: mellard@msu.edu, mellard@ku.edu (J.P. Mellard), kyoshiyama@ori.u-tokyo.ac.jp (K. Yoshiyama), litchman@msu.edu (E. Litchman), klausme1@msu.edu (C.A. Klausmeier).

0022-5193/$ - see front matter © 2010 Elsevier Ltd. All rights reserved.
doi:10.1016/j.jtbi.2010.09.041

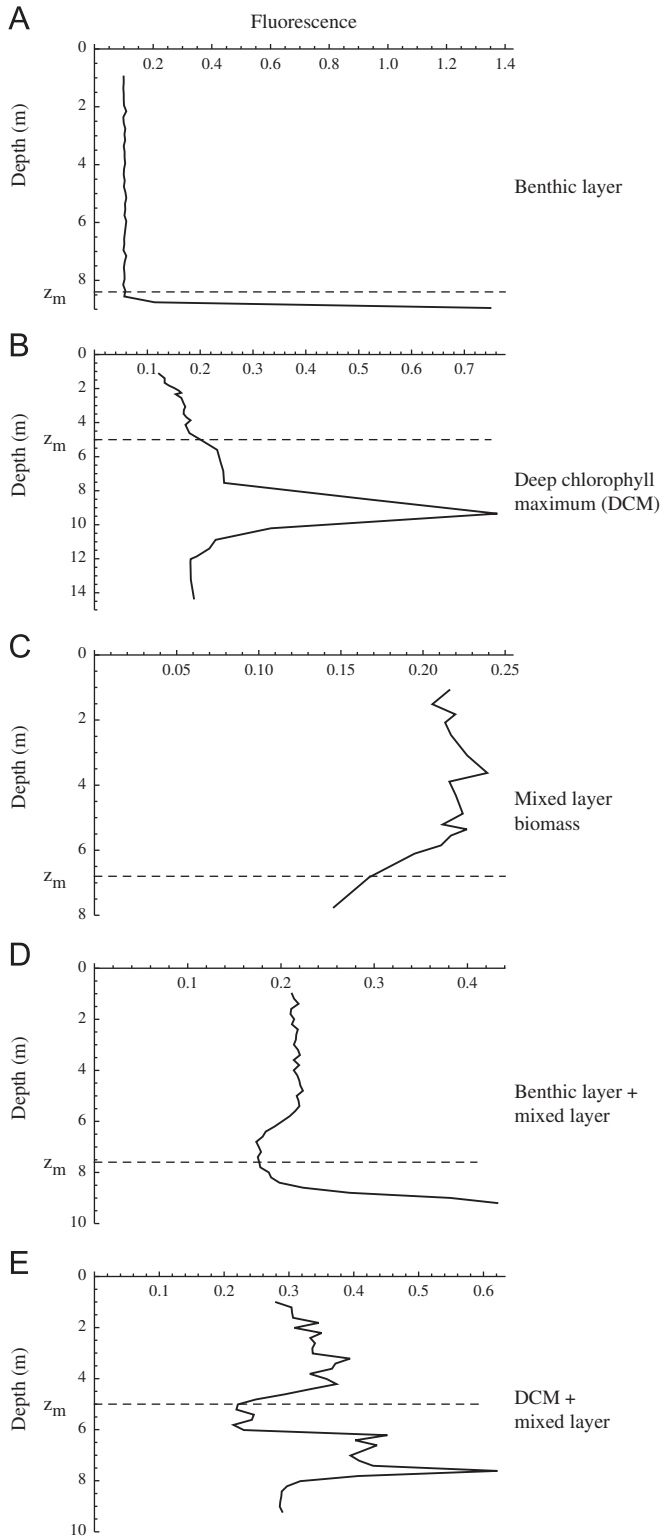

Fig. 1. Examples of phytoplankton vertical distributions observed in stratified lakes in Southern Michigan. (A) Benthic layer biomass only. (B) DCM biomass only. (C) Mixed layer biomass only. (D) Benthic layer and mixed layer biomass. (E) DCM and mixed layer biomass. Vertical distributions are chlorophyll *a* fluorescence profiles and mixed layer depth, z_m, is defined from the temperature profile to be the depth 1 °C cooler than the surface temperature. Profile (A) is from Sherman Lake, Kalamazoo County MI, October 12, 2007. Profile (B) is from Bristol Lake, Barry County MI, October 3, 2007. Profile (C) is from Fine Lake, Barry County MI, October 3, 2007. Profile (D) is from Hogsett Lake, Kalamazoo County MI, October 22, 2007. Profile (E) is from Bassett Lake, Barry County MI, October 15, 2007.

experience varying local light levels and therefore varying growth rates. The light level at the bottom of the water column, I_{out}, predicts the outcome of competition for light (Huisman and Weissing, 1994, 1995) in a way similar to R^* for nutrients (Tilman, 1982). In contrast, in a poorly mixed water column, motile phytoplankton can be thought of as playing a competitive game in opposing essential resource gradients. A shallower position allows a cell to shade those below it but a deeper position allows it to intercept nutrients mixing up from below. Eventually, through movement and/or growth, phytoplankton will aggregate at their evolutionarily stable strategy (ESS) depth z^*, which is the depth of equal limitation by nutrients and light and prevents growth elsewhere in the water column (Klausmeier and Litchman, 2001). These studies are applicable to the two extremes of whole water columns, one of well-mixed and one of poorly mixed.

Many bodies of water stratify. Several models have considered stratified water columns, ranging from complex simulation models particular to specific ecosystems (Lucas et al., 1998; Fennel and Boss, 2003; Peeters et al., 2007; Ross and Sharples, 2007) to simpler models aimed at general understanding. Condie and Bormans (1997) and Hodges and Rudnick (2004) included sinking but neglect the feedback of phytoplankton on light. Huisman and Sommeijer (2002a,b) incorporate the feedback of phytoplankton on light, but omit nutrients and assume no mixing in the hypolimnion. Yoshiyama and Nakajima (2002), Yoshiyama et al. (2009), and Ryabov et al. (2010) do not include nutrient loading to the mixed layer. Our study systematically explores the different vertical distributions of phytoplankton that can arise from intraspecific competition for nutrients and light in a stratified water column.

In this paper, we build on previous work by considering a stratified water column with a well-mixed surface layer on top of a poorly mixed deep layer, a combination of approaches by Huisman and Weissing (1994, 1995) and Klausmeier and Litchman (2001). We relax the assumption of an infinitely thin layer (Klausmeier and Litchman, 2001) to a mixed layer of finite depth and show what resources limit growth at different depths within the layer. Furthermore, we consider multiple nutrient inputs, including input directly to the mixed layer, expanding on Diehl (2002). Current models for poorly mixed water columns consider only nutrient supply from below (Klausmeier and Litchman, 2001; Huisman et al., 2006; Beckmann and Hense, 2007). We enumerate the possible equilibrium algal vertical strategies and show under what conditions each should occur.

2. Methods

2.1. Full model

The full model consists of partial differential equations for biomass, $b(z,t)$ and nutrients, $R(z,t)$ which in our examples represents phosphorus, and an integral equation for light, $I(z,t)$. We consider a one-dimensional water column where z is depth with the surface at $z=0$ and the bottom at $z=z_b$.

Phytoplankton biomass b grows according to Liebig's law of the minimum, so gross growth rate at depth z is $g(R,I) = \min(f_I(I(z,t)),f_R(R(z,t)))$. Functions $f_I(I)$ and $f_R(R)$ are the potential growth rates as a function of the resource I or R when that resource is limiting. We use the Michaelis–Menten form for the functions in our numerical solutions, $f_I(I)=rI/(I+K_I)$ and $f_R(R)=rR/(R+K_R)$ where r is the maximum growth rate and K_I and K_R are half-saturation constants for light and nutrients, respectively. Our qualitative results, however, should hold for other bounded, strictly increasing functions. Biomass is lost at density independent rate m, which encompasses all sources of mortality. Net

growth rate is $g(z)-m$. Net growth at depth z is only possible if both I is greater than the break even light level, $I^*=f_I^{-1}(m)$, and R is greater than the break even nutrient concentration, $R^*=f_R^{-1}(m)$ (Tilman, 1982).

A depth-dependent turbulent eddy diffusion coefficient $D(z)$ describes passive movement. Active movement is described by a taxis term (Okubo, 1980). Phytoplankton behavior is governed by simple rules. They move up if conditions immediately above are better than immediately below, move down if conditions immediately below are better than immediately above, and do not move if conditions are worse immediately above and below. To describe this behavior, we let phytoplankton velocity v depend on the gradient in growth rate, $\partial g/\partial z$. We assume v to be an odd decreasing function that approaches $v_{\max}$ as $\partial g/\partial z$ approaches negative infinity (positive v is upward), approaches $-v_{\max}$ as $\partial g/\partial z$ approaches positive infinity, and $v(0)=0$. See the section titled Assumptions, limitations, and extensions in the Discussion for how relaxing the assumption of active motility affects results.

Change in biomass at depth z is the balance of growth, death, and passive and active movement:

$$\frac{\partial b}{\partial t}=(g(R,I)-m)b+\frac{\partial}{\partial z}\left(D(z)\frac{\partial b}{\partial z}+v\left(\frac{\partial g}{\partial z}\right)b\right). \quad (1)$$

Nutrients R are taken up by phytoplankton with a yield of Y biomass per unit nutrient consumed, are mixed with eddy diffusion coefficient $D(z)$, are supplied directly to the water column at depth z at rate $R_{\text{in}}(z)$, and are recycled from dead phytoplankton with proportion ε:

$$\frac{\partial R}{\partial t}=-g(R,I)\frac{b}{Y}+\frac{\partial}{\partial z}\left(D(z)\frac{\partial R}{\partial z}\right)+R_{\text{in}}(z)+\varepsilon m\frac{b}{Y}. \quad (2)$$

Light follows Lambert–Beer's law, decreasing due to attenuation from biomass and background turbidity (Kirk, 1975). The attenuation coefficient due to biomass is a and due to background is a_{bg}:

$$I(z,t)=I_{\text{in}}e^{-(a_{\text{bg}}z+\int_0^z ab(Z,t)\,dZ)}. \quad (3)$$

Phytoplankton do not leave or enter the water column, so boundary conditions are

$$\left(D(z)\frac{\partial b}{\partial z}+v\left(\frac{\partial g}{\partial z}\right)b\right)\Big|_{z=0,z_{\text{b}}}=0. \quad (4)$$

Nutrients have no surface flux but diffuse into the water column from the sediments where they have fixed concentration R_{sed} at a rate proportional to the concentration difference across the interface. The permeability of the interface is described by h.

$$\frac{\partial R}{\partial z}\Big|_{z=0}=0 \quad \text{and} \quad \frac{\partial R}{\partial z}\Big|_{z=z_{\text{b}}}=h(R_{\text{sed}}-R(z_{\text{b}})). \quad (5)$$

See Table 1 for a list of parameters and their default values.

2.1.1. Simulating the full model

The system of reaction–diffusion equations that define our model (Eqs. (1)–(5)) defies analytical treatment, so we begin with numerical solutions of the model to gain insight into its behavior. We spatially discretized and numerically simulated the full model using VODE (Brown et al., 1989) following Huisman and Sommeijer (2002b). The specific equation we use for v is $v=-v_{\max}\cdot\partial g/\partial z/(|\partial g/\partial z|+K_{\text{swim}})$, where $K_{\text{swim}}=0.001\,\text{m}^{-1}\,\text{d}^{-1}$. We simulate a stratified water column with mixed layer depth z_{m}, setting $D(z)=10^2\,\text{m}^2\,\text{d}^{-1}$ for $0\le z\le z_{\text{m}}$ and $D(z)=1\,\text{m}^2\,\text{d}^{-1}$ for $z_{\text{m}}<z\le z_{\text{b}}$, realistic values for $D(z)$ in the epilimnion and hypolimnion (MacIntyre et al., 1999). An example equilibrium vertical profile shows that biomass is almost uniformly distributed in the mixed layer and forms a deep chlorophyll maximum (DCM) in the deep layer (Fig. 2A). The DCM thickness

Table 1
Variables and parameter values unless noted otherwise.

Variable or parameter	Value (range)	Units	Meaning	Reference
$b(z,t)$		cells mL^{-1}	Biomass concentration	
B_{ML}		cells cm^{-2}	Biomass in ML	
B_{DL}		cells cm^{-2}	Biomass in DL	
z^*		m	Depth of co-limitation in DL	
z_{e}		m	Depth of co-limitation in ML	
$R(z,t)$		$\mu\text{g P L}^{-1}$	Phosphorus concentration	
$\overline{R}_{\text{ML}}$		$\mu\text{g P L}^{-1}$	Average phosphorus concentration in ML	
$I(z,t)$		$\mu\text{mol photons m}^{-2}\,\text{s}^{-1}$	Irradiance	
$g(R,I)$		d^{-1}	Growth rate	
$\overline{g}_{\text{ML}}$		d^{-1}	Average growth rate in ML	
r	0.4	d^{-1}	Maximum growth rate	(1)
m	0.2	d^{-1}	Loss rate	(1)
K_R	1.0	$\mu\text{g P L}^{-1}$	Phosphorus half-saturation constant	(1)
K_I	50.0	$\mu\text{mol photons m}^{-2}\,\text{s}^{-1}$	Light half-saturation constant	(1)
Y	10^3	cells mL^{-1} $[\mu\text{g P L}^{-1}]^{-1}$	Yield coefficient	(1)
D_{DL}	1.0	$\text{m}^2\,\text{d}^{-1}$	Diffusion coefficient in deep layer	(1,2)
I_{in}	1400	$\mu\text{mol photons m}^{-2}\,\text{s}^{-1}$	Incoming light	(1)
a_{bg}	0.1 (10^{-2}–10)	m^{-1}	Background attenuation coefficient	(1,4)
a	10^{-5}	m^{-1} $[\text{cells mL}^{-1}]^{-1}$	Algal attenuation coefficient	(1,4)
z_{b}	20 (1–10^3)	m	Water column depth	(1,5)
z_{m}	5 (0–z_{b})	m	Mixed layer depth	(5)
R_{sed}	10 (0–10^3)	$\mu\text{g P L}^{-1}$	Sediment phosphorus concentration	(1,3,5,6)
h	10^{-2}	m^{-1}	Sediment–water column interface permeability	(1)
ε	0.9	Dimensionless	Recycling coefficient	(1,7,8)
$v_{\max}$	10	m d^{-1}	Swimming speed	(1)
R_{inML}	1 (0–10^2)	$\text{mg P m}^{-2}\,\text{d}^{-1}$	Mixed layer nutrient input	(9,10)

Sources: (1) Klausmeier and Litchman (2001). (2) MacIntyre et al. (1999). (3) Jöhnk et al. (2008). (4) Krause-Jensen and Sand-Jensen (1998). (5) Wetzel (1975). (6) Portielje and Lijklema (1999). (7) Peters and Rigler (1973). (8) Depinto and Verhoff (1977). (9) Gonsiorczyk et al. (1998). (10) Sharpley et al. (1996). Ranges explored here are in parentheses.

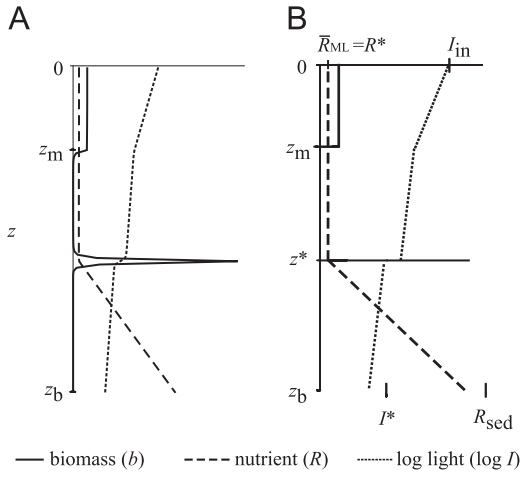

Fig. 2. (A) Examples of predictions of the full model showing a DCM and nutrient-limited mixed layer at steady-state. Solid line is biomass (cells mL^{-1}), dashed line is nutrient concentration (μg dissolved PL^{-1}), and dotted line is log light (μmol photons $m^{-2}\,s^{-1}$). Parameters are as in Table 1 except $R_{sed}=220\ \mu g\,P\,L^{-1}$; $D_{ML}=10^2\ m^2\ \ d^{-1}$; $R_{in}(z)=0.6\ \mu g\,P\,L^{-1}\,d^{-1}$ for $0\le z\le 5, R_{in}(z)=0$ for $z>5$. (B) Example representation of simplified model showing a DCM and nutrient-limited mixed layer as in the output of the full model.

decreases as the swimming speed of the phytoplankton is increased until it can be approximated by an infinitely thin layer (Klausmeier and Litchman, 2001; Du and Hsu, 2008). Nutrients are almost uniformly distributed in the mixed layer, relatively constant below the mixed layer down to the DCM, and increase linearly below the DCM to the sediments. These numerical results and previous research (Huisman and Weissing, 1994; Klausmeier and Litchman, 2001) suggest that the full model can be approximated by a simplified model (Fig. 2B) with a completely homogenous mixed layer above a poorly mixed layer where phytoplankton can form a thin layer.

2.2. Simplified model

In order to obtain analytical results, we use a simplified model to approximate the equilibrium distribution of the full model. Evidence that the full model can be reduced to a simpler model comes from simulations (Klausmeier and Litchman, 2001) and a rigorous mathematical proof (Du and Hsu, 2008). We later give criteria for when our simplified model does a good job of approximating the full model as well as discuss specific cases for when it may do a poor job (see Section 4.1).

In addition to providing intuitive insight, algebraic expressions, and ease of numerically exploring parameter space, the simplified model provides a skeleton of the full model showing where the peaks in biomass occur, the depth of co-limitation, and the amount of biomass in the mixed layer and deep layer (compare Fig. 2B with Fig. 2A). We break up the water column into a perfectly mixed layer (Huisman and Weissing, 1994) and a poorly mixed deep layer (Klausmeier and Litchman, 2001). This water column approximates stratified temperate lakes (Wetzel, 1975; Wüest et al., 2000) and oceans (Osborn, 1980; Mann and Lazier, 1996).

2.2.1. Definitions and assumptions

Well-mixed surface layer (ML): In the mixed layer, $0\le z\le z_m$, we assume $D(z)$ is large enough to homogenize the nutrients and phytoplankton, overcoming phytoplankton motility, growth, and nutrient consumption ($D(z)\gg v_{max}z_m$ and $D(z)\gg gz_m^2$ for $0\le z\le z_m$). Phytoplankton and nutrient distributions observed in thermally stratified lakes are often consistent with this assumption (Fig. 1).

Define B_{ML} to be the depth-integrated biomass in the mixed layer

$$B_{ML}=\int_0^{z_m} b(z)\,dz \tag{6}$$

and $\overline{R}_{ML}$ to be the average nutrient concentration in the mixed layer

$$\overline{R}_{ML}=\frac{1}{z_m}\int_0^{z_m} R(z)\,dz. \tag{7}$$

To explore the effect of changing z_m without changing the nutrient supply to the mixed layer, we assume the only source of nutrients besides the sediments is direct surface input by setting $R_{in}(z)$ as a delta function at $z=0$ with total nutrient input rate R_{inML}

$$R_{inML}=\int_0^{z_m} R_{in}(z)\,dz. \tag{8}$$

Define $\overline{g}_{ML}$ to be the average growth rate in the mixed layer

$$\overline{g}_{ML}=\frac{1}{z_m}\int_0^{z_m} g(z)\,dz \tag{9}$$

and z_e to be the depth of equal limitation where

$$f_R(R(z_e))=f_I(I(z_e)). \tag{10}$$

Poorly mixed deep layer (DL): In the deep layer, $z_m<z\le z_b$, we assume that phytoplankton motility or growth can overcome mixing to form a thin layer ($v_{max}(z_b-z_m)\gg D(z)$ or $g(z_b-z_m)^2\gg D(z)$ for $z_m<z\le z_b$). Following Klausmeier and Litchman (2001), we assume that algae will aggregate at their ESS depth z^*. Note that there are two ways for the algae to achieve their ESS depth z^*. According to the inequalities, either swimming or growth can overcome mixing. For a DCM, $z_e=z^*$. We use a delta function to approximate the biomass distribution at depth z^* (Klausmeier and Litchman, 2001),

$$b(z)=B_{DL}\delta(z^*), \tag{11}$$

where depth integrated biomass in the deep layer is

$$B_{DL}=\int_{z_m}^{z_b} b(z)\,dz. \tag{12}$$

2.2.2. Equilibrium conditions

We focus on vertical distribution at both dynamic ($d/dt=0$) and strategic (ESS) equilibrium. At equilibrium, net growth rate is 0 wherever biomass exists

$$\begin{cases}\overline{g}_{ML}-m=0 & \text{if } B_{ML}>0,\\ g(z^*)-m=0 & \text{if } B_{DL}>0.\end{cases} \tag{13}$$

In other words, at equilibrium, if the population exists in the mixed layer or deep layer, it is neither increasing or decreasing there. For an equilibrium to be an ESS,

$$\begin{cases}\overline{g}_{ML}-m\le 0 & \text{and}\\ g(z)-m\le 0 & \text{for } z_m<z\le z_b.\end{cases} \tag{14}$$

In other words, phytoplankton cannot invade the mixed layer or deep layer.

Steady states of the simplified model consist of the following state variables: B_{ML}, $\overline{R}_{inML}$, B_{DL}, and z^* (if $B_{DL}>0$). Derivation of steady states is shown in the Appendix. Stability of steady states is evaluated by conditions (14).

3. Results

3.1. Spatial distribution states

Stratification and multiple nutrient sources lead to a greater diversity of possible equilibrium vertical distributions and resource limitation states of phytoplankton than in previous models. In the mixed layer, four states for phytoplankton are possible: light-limited ($f_R(z) > f_I(z)$ for $0 \le z \le z_m$), nutrient-limited ($f_R(z) < f_I(z)$ for $0 \le z \le z_m$), co-limited ($0 \le z_e \le z_m$), or not present (empty). In the deep layer, three states for phytoplankton are possible: nutrient-limited in a benthic layer, co-limited in a deep chlorophyll maximum, or not present (empty). Combinations of these four mixed layer and three deep layer biomass states result in $4 \times 3 = 12$ conceivable vertical distribution states. However, four of these vertical distribution states are infeasible. In order to have both mixed layer and deep layer biomass, the mixed layer biomass must be nutrient-limited (if mixed layer biomass is co-limited or light-limited then the light level below the mixed layer is less than I^*). This eliminates the four combinations of co-limited or light-limited mixed layer biomass states with any deep layer biomass state, leaving eight possible vertical distribution states at equilibrium (for proof see Appendix).

3.2. Possible distribution states

There is often appreciable nutrient input directly to the mixed layer, due to riverine inputs, surface runoff, or atmospheric deposition. This mixed layer nutrient input, R_{inML}, can depend on landscape geomorphology and anthropogenic influences surrounding the body of water. Here we consider the case $R_{inML} > 0$, although some kettle or other glacial lakes that have very small drainage basins might be reasonably approximated by an assumption of no mixed layer nutrient input (Hutchinson, 1957).

With mixed layer nutrient input, six equilibrium vertical distribution states are possible (Fig. 3). A benthic layer or DCM by itself are not possible with positive R_{inML}, because any amount of nutrient input to the mixed layer will sustain a mixed-layer population (see Section 3.2.1). We describe the equilibrium vertical distribution states below; mathematical details are given in the Appendix.

(1) *Empty.* An empty state is perhaps trivial because likely all bodies of water have enough nutrients for some biomass to exist but we describe it here as a possibility. No biomass persists in the water column. Light declines exponentially with depth due to background attenuation. Nutrient levels are uniform with depth and at the same concentration as in the sediments ($R(z) = R_{sed}$). See Fig. 3A and Case 1 in the Appendix.

(2) *Co-limited mixed layer.* A co-limited mixed layer is actually only co-limited at one depth in the mixed layer, but as a whole, we consider it co-limited because the population experiences both nutrient-limited and light-limited conditions in the mixed layer. Biomass is uniformly distributed throughout the mixed layer and absent below it. The upper portion of the mixed layer ($z < z_e$) is nutrient-limited and the lower portion ($z > z_e$) is light-limited. Light declines exponentially within the mixed layer due to algal and background attenuation and in the deep layer below due to background attenuation only. Light at the bottom of the mixed layer is actually less than the break-even level ($I(z_m) = I_{out} \le I^*$), but the population can persist (Huisman and Weissing, 1994). Nutrients in the mixed layer are uniform at or above the break-even concentration ($\bar{R}_{ML} \ge R^*$) and increase linearly with depth in the deep layer. See Fig. 3B and Case 2 in the Appendix.

(3) *Light-limited mixed layer.* In a light-limited mixed layer, conditions are the same as a co-limited mixed layer except the entire mixed layer is limited by light ($f_R(\bar{R}_{ML}) > f_I(I_{in})$). See Fig. 3C and Case 3 in the Appendix.

(4) *Nutrient-limited mixed layer.* A nutrient-limited mixed layer by itself may be somewhat unlikely as most bodies of water have sufficient nutrient input from the sediments to sustain population growth in the deep layer as well. Conditions are the same as co-limited and light-limited mixed layers except nutrients in the mixed layer are at the break even concentration ($\bar{R}_{ML} = R^*$) and below the mixed layer, are constant or

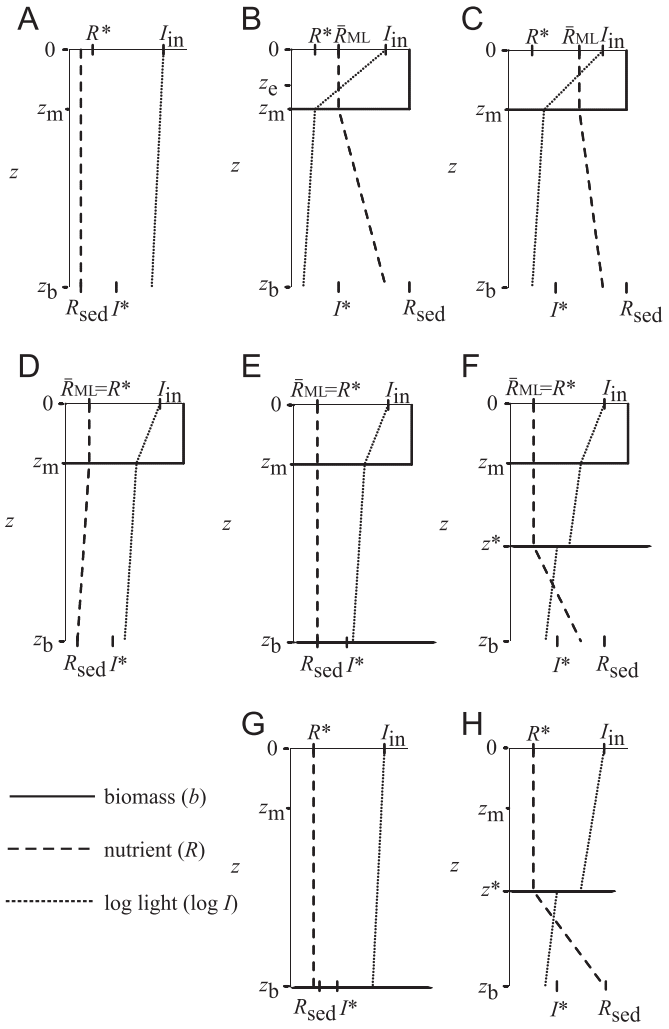

Fig. 3. Equilibrium vertical profiles (A)–(F) with mixed layer nutrient input ($R_{inML} > 0$). (G) and (H) are special cases where $R_{inML} = 0$. (A) Empty. Here, there is not sufficient nutrients for biomass to persist. (B) Co-limited mixed layer. The solid lines enveloping the mixed layer represents the biomass there. $\bar{R}_{ML}$ is the nutrient concentration in the mixed layer. (C) *I*-Light-limited mixed layer. The mixed layer biomass is completely light-limited due to increased R_{sed}. (D) Nutrient-limited mixed layer. Primary nutrient source is directly to the mixed layer ($R_{sed} < R^*$). The entire mixed layer is nutrient limited because $I(z_m) > I^*$. (E) Benthic layer and nutrient-limited mixed layer (BL+ML). The solid line at the bottom represents biomass in the benthic layer. $I(z_b^+) > I^*$. $R = R^*$ in both layers. (F) DCM and nutrient-limited mixed layer. The solid line representing biomass in the DCM is at z^*, where $R = R^*$ and $I(z^{*+}) = I^*$. $R = R^*$ in both layers (DCM+ML). (G) Benthic layer. The solid line at the bottom represents biomass in the benthic layer. There are enough nutrients at the sediment ($R_{sed} > R^*$) and enough light ($I(z_b^+) > I^*$) for biomass to exist at the bottom of the water column. Nutrients above the benthic layer are constant at R^*. (H) DCM. The solid line representing biomass in the DCM is at z^*, where $R = R^*$ and $I = I^*$.

decrease linearly to $R(z_b)$. See Fig. 3D and Case 4 in the Appendix.

(5) *Benthic layer + nutrient-limited mixed layer* (BL+ML). This is an intriguing case with the population divided between two depths but with both depths limited by the same resource. Biomass is uniformly distributed throughout the mixed layer and resides at the sediment–water interface in the deep layer. The entire mixed layer and the benthic layer are limited by nutrients. Light declines exponentially with depth in the mixed layer due to algal and background attenuation and in the deep layer below due to background attenuation only. Light at the bottom of the water column $I(z_b) > I^*$. Nutrients are uniformly distributed throughout the water column at the break-even concentration ($R(z)=R^*$). See Fig. 3E and Case 5 in the Appendix.

(6) *Deep chlorophyll maximum+nutrient-limited mixed layer* (DCM+ML). This is another intriguing and probably common (Mellard, 2010) case. Biomass is uniformly distributed throughout the mixed layer and forms a thin layer at depth z^* within the deep layer. The entire mixed layer is limited by nutrients and the DCM is limited by nutrients and light. Light declines exponentially with depth in the mixed layer due to algal and background attenuation. In the deep layer, light declines exponentially above and below the DCM and decreases a finite amount within the DCM. Immediately below z^*, light is at the break-even level ($I(z^{*+})=I^*$). Nutrients in the mixed layer and below to the DCM are constant at R^*. Below the DCM, nutrients increase linearly with depth. See Fig. 3F and Case 6 in the Appendix.

3.2.1. *Two special cases if $R_{inML}=0$*

Benthic layer and DCM are special cases of BL+ML and DCM+ML where $R_{inML}=0$.

(7) *Benthic layer* (BL). The benthic layer is the only depth in the water column the population exists in this case. Biomass resides at the sediment–water interface at $z=z_b$. Light declines exponentially with depth due to background attenuation and there is sufficient light at the bottom ($I(z_b) > I^*$). Nutrient levels are uniform throughout the water column at R^*. See Fig. 3G and Case 7 in the Appendix.

(8) *Deep chlorophyll maximum* (DCM). The conspicuous DCM (Camacho, 2006) is considered to form at the ESS depth (of co-limitation) in the deep layer. Biomass forms a thin layer at depth z^* within the deep layer. Light declines exponentially above and below the DCM and decreases a finite amount at the DCM. Immediately below z^*, $I(z^{*+})=I^*$. Nutrient levels are at R^* at and above the DCM and increase linearly below the DCM. See Fig. 3H and Case 8 in the Appendix.

3.3. *Transitions along environmental gradients*

We now examine how the equilibrium vertical distribution, biomass, and resource limitation depend on environmental parameters. We focus on four environmental parameters that are known to vary among water bodies or through time and that potentially affect phytoplankton communities: sediment nutrient concentration, R_{sed}; mixed layer nutrient input, R_{inML}; background light attenuation, a_{bg}; and mixed layer depth, z_m. Sediment nutrient concentration varies widely between lakes. Background light attenuation depends on the amount and composition of particulate and dissolved matter suspended in the water column. Mixed layer depth can vary both between and within bodies of water through time due to seasonal changes (Wetzel, 1975). Note that other transitions are possible than what are described below.

Effect of sediment nutrient concentration. Nutrient enrichment in the form of sediment nutrient concentration causes phytoplankton to shift towards the surface. For example, in Fig. 4A, they shift from a BL+ML to a DCM+ML to a co-limited mixed layer to a completely light-limited mixed layer. Increasing R_{sed} pushes z^* and z_e towards the surface as the biomass becomes more light-limited. Total biomass increases until it is light-limited. Interestingly, the nutrient-limited mixed layer biomass is unaffected by increasing sediment nutrient concentration because the deep layer biomass uses it all for growth.

Effect of mixed layer nutrient input. Nutrient enrichment in the form of mixed layer nutrient input causes phytoplankton to shift towards the surface. For example, in Fig. 4B, they shift from a BL+ML to a DCM+ML to a co-limited mixed layer to a light-limited mixed layer. Increasing R_{inML} pushes z^* and z_e towards the surface as the biomass becomes more light limited. Total biomass steadily increases, but solely due to mixed layer biomass increasing: benthic layer biomass does not increase and DCM biomass actually slightly decreases with increasing R_{inML}.

Effect of background light attenuation. Increases in background light attenuation causes phytoplankton to shift towards the surface. For example, in Fig. 4C, the phytoplankton shift from a BL+ML to a DCM+ML to a co-limited mixed layer to a light-limited mixed layer before eventually going extinct. Increasing a_{bg} pushes z^* and z_e towards the surface as the biomass becomes more light-limited. Increasing a_{bg} has no effect on completely nutrient-limited biomass (benthic layer or nutrient-limited mixed layer). However, for all other states, increasing a_{bg} decreases biomass.

Effect of mixed layer depth. Increases in mixed layer depth can cause phytoplankton to shift towards the surface due to entrainment once $z_m \geq z^*$. For example, in Fig. 4D, the phytoplankton shift from a DCM+ML to a co-limited mixed layer once the mixed layer entrains the DCM to a light-limited mixed layer and finally to an empty state when the mixed layer becomes too deep and the phytoplankton go extinct because of extreme light limitation. Increasing z_m has no effect on z^* for the DCM; however, z_e for the co-limited mixed layer becomes shallower with increasing mixed layer depth (although this is not universally true). Increasing mixed layer depth has negative, positive, or no effect on biomass, dependent on the state of the phytoplankton. Biomass in a BL, DCM, or nutrient-limited mixed layer (when a BL or DCM is present) is unaffected by increasing mixed layer depth. Biomass in a light-limited or nutrient-limited mixed layer (by itself) decreases with increasing mixed layer depth. Biomass in a co-limited mixed layer may increase or decrease with increasing mixed layer depth.

Interactive effects of environmental parameters. The vertical distribution as a function of R_{sed} and R_{inML} is shown in Fig. 5. Increasing either of these parameters makes the phytoplankton more light-limited so that these parameters jointly determine vertical distribution. The difference between increasing either of these two parameters is subtle and not illustrated in Fig. 5 but can be seen by comparing Figs. 4A and B. When biomass is present in both layers, each exhibits asymmetric control over the nutrient sources so that only mixed layer biomass increases if R_{inML} increases and only deep layer biomass increases if R_{sed} increases.

The vertical distribution as a function of a_{bg} and z_m is shown in Fig. 6. Increasing either of these parameters makes the phytoplankton more light-limited as well, however, these parameters interact to determine vertical distribution. Interestingly, the transition from a benthic layer (BL+ML) to a deep chlorophyll maximum (DCM+ML) is not affected by mixed layer depth. Other states show non-unidirectional relationships (co-limited ML). All four environmental parameters may interact to determine vertical distribution. Overall, these four parameters,

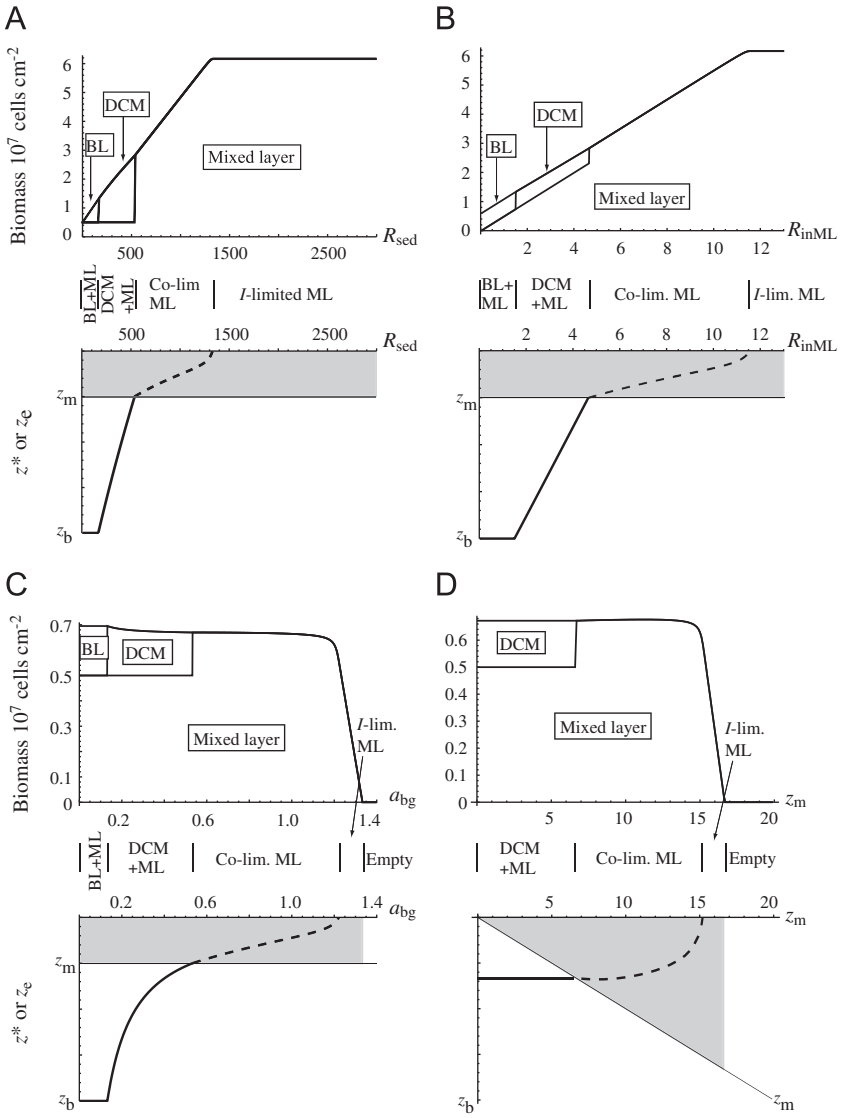

Fig. 4. Effect of environmental parameter on phytoplankton biomass and vertical distribution. (Top) Amount of biomass in benthic layer (BL), DCM, and mixed layer. (Middle) State of the phytoplankton. Phytoplankton can be in a benthic layer + nutrient-limited mixed layer (BL+ML), DCM + nutrient-limited mixed layer (DCM+ML), co-limited mixed layer (Co-lim. ML), light-limited mixed layer (*I*-lim. ML), or extinct (Empty). (Bottom) Dotted line is depth of colimitation if in the mixed layer, z_e, and solid line is depth of colimitation if in the deep layer, z^*. Gray shading indicates that biomass is present in the mixed layer. (A) Effect of sediment phosphorus concentration, R_{sed}, on phytoplankton biomass and vertical distribution. Environmental parameters: $a_{bg}=0.1\,m^{-1}$; $z_m=5\,m$; $R_{inML}=1\,mg\,P\,m^{-2}\ d^{-1}$. (B) Effect of R_{inML} on phytoplankton biomass and vertical distribution. Environmental parameters: $a_{bg}=0.1\,m^{-1}$; $z_m=5\,m$; $R_{sed}=120\,\mu g\,P\,L^{-1}$. (C) Effect of a_{bg} on phytoplankton biomass and vertical distribution. Environmental parameters: $z_m=5\,m$; $R_{sed}=40\,\mu g\,P\,L^{-1}$; $R_{inML}=1\,mg\,P\,m^{-2}\ d^{-1}$. (D) Effect of z_m on phytoplankton biomass and vertical distribution. Environmental parameters: $a_{bg}=0.4\,m^{-1}$; $R_{sed}=40\,\mu g\,P\,L^{-1}$; $R_{inML}=1\,mg\,P\,m^{-2}\ d^{-1}$.

either individually or combined, shift the phytoplankton to more light-limited conditions if increased (results not shown).

4. Discussion

Aquatic communities exhibit pronounced spatial patterns (Steele, 1978). How competition structures the spatial distributions of organisms through feedbacks in abiotic and biotic components is important to understanding how biological heterogeneity is generated. We have shown how externally imposed heterogeneity in the form of resource gradients and mixing interacts with internally generated heterogeneity in the form of competition, population dynamics, and movement to determine the spatial distribution of phytoplankton.

Our simplified model is like an X-ray that exposes the skeleton upon which the vertical distributions of phytoplankton are fleshed out. It also incorporates two important components of the phytoplankton environment required to replicate real patterns in aquatic systems. First, we add stratification, which creates spatially varying mixing, expands a thin layer to finite thickness in the mixed layer, and allows for different relative resource limitation within the mixed layer. Second, we add multiple nutrient sources, which can create multi-modal phytoplankton distributions.

The inclusion of stratification means that in our simplified model, phytoplankton can exist at a single depth such as in a DCM or benthic layer, or can be homogeneously distributed throughout the mixed layer. In a DCM in a poorly mixed water column, phytoplankton exist in a thin layer at their depth of equal

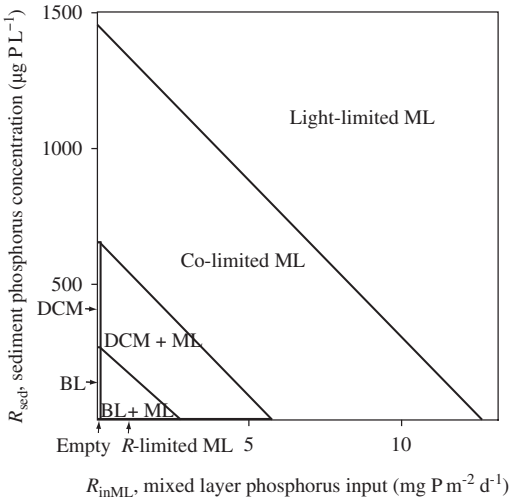

Fig. 5. Two-dimensional bifurcation plot of sediment phosphorus concentration, R_{sed}, and mixed layer nutrient input, R_{inML}. Note that the benthic layer and DCM regions lie directly on the R_{sed} axis ($R_{inML}=0$). Environmental parameters: $a_{bg}=0.1\,m^{-1}$; $z_m=5\,m$.

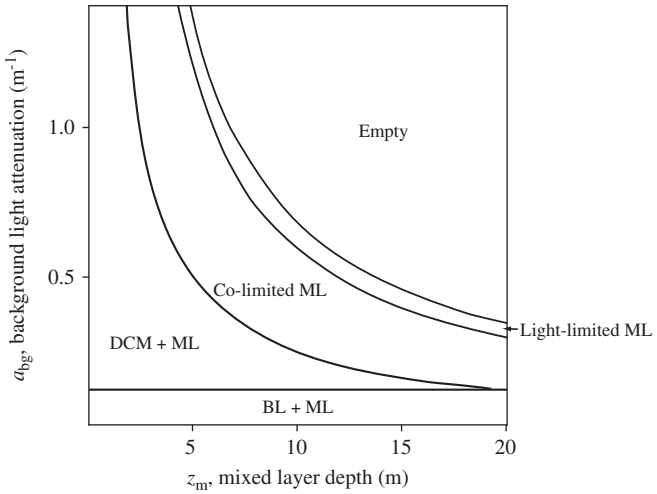

Fig. 6. Two-dimensional bifurcation plot of background light attenuation, a_{bg}, and mixed layer depth, z_m. Increases in both parameters can lead to extinction. Environmental parameters: $R_{sed}=200\,\mu g\,P\,L^{-1}$; $R_{inML}=0.1\,mg\,P\,m^{-2}\,d^{-1}$.

limitation by nutrients and light, z^* (Klausmeier and Litchman, 2001). However, when the depth of equal limitation occurs within the mixed layer, the thin layer is expanded to the thickness of the mixed layer and phytoplankton exist above and below the depth of equal limitation. Decreasing the mixed layer depth to zero in our model reveals a subtle mistake in the surface scum case of Klausmeier and Litchman (2001). They erroneously neglect the inevitable spatial gradient in light in a surface scum and conclude that a surface scum must be light-limited. Our current analysis shows this is not the case, because a surface scum may be co-limited over a range of R_{sed}. We also correct the formulas for biomass in this case (see Case 2 in the Appendix).

One of the intriguing results of our study is the possibility of phytoplankton biomass to maintain source populations in both the mixed layer and deep layer simultaneously. Without nutrient input directly to the mixed layer, a phytoplankton population can grow either only in the mixed layer or only in the deep layer. However, when there is nutrient input directly to the mixed layer, phytoplankton populations can grow in the mixed layer and in the deep layer together. This bimodal distribution occurs not merely due to passive dispersal from a source habitat into a sink habitat, but instead because growing conditions are favorable in these two depths. Phytoplankton in the mixed layer and deep layer is a common feature in many lakes (Fig. 1, Mellard, 2010), which may be explained as the adaptive response of phytoplankton to multiple nutrient inputs to the water column. One alternative explanation is the coexistence of two species exhibiting a trade-off in their light and nutrient requirements that competitively divide the water column into separate niches (Yoshiyama et al., 2009); another alternative explanation is passive dispersal from a source to a sink habitat.

Other studies that have considered stratification have also found interesting results such as bistability of biomass between the mixed layer and deep layer (Yoshiyama and Nakajima, 2002; Ryabov et al., 2010) and biomass straddling both layers simultaneously due to sinking or actual production in both layers (Huisman and Sommeijer, 2002b; Hodges and Rudnick, 2004; Beckmann and Hense, 2007; also mentioned as a possibility in Ryabov et al., 2010). Although our results do not show bistability of biomass distributions, we do see that in some area of parameter space, a small change in a parameter can cause a major shift in phytoplankton vertical distribution. For example, in Figs. 4A and C, over a small range of R_{sed} and a_{bg}, respectively, the DCM can shift many meters or the population can even change to a different vertical distribution state. Many bodies of water may exist in this range in parameter space since many have DCMs (Camacho, 2006; Mellard, 2010). This could have important ramifications for the sensitivity of those bodies of water to environmental change.

The presence of a mixed layer adds complications that few studies have explored thoroughly (Beckmann and Hense, 2007, but see Yoshiyama et al., 2009; Ryabov et al., 2010). The particular form of depth-dependent mixing may influence results. Previous studies have used many different forms ranging from no mixing in the deep layer (Huisman and Sommeijer 2002a,b) to a step function (Hodges and Rudnick, 2004; Yoshiyama et al., 2009), to a smoothly varying thermocline (Yoshiyama et al., 2009; Ryabov et al., 2010) to a thermocline region with reduced diffusivities (Yoshiyama and Nakajima, 2002). Future studies should examine the influence that the particular form of stratification has on results.

4.1. Assumptions, limitations, and extensions

Our simplified model assumes that mixing is strong enough to homogenize the phytoplankton and nutrients in the mixed layer, while mixing is very weak in the deep layer. In general, our inequalities guide the conditions under which our simplified model approximates the full model ($D(z) \gg v_{max} z_m$ and $D(z) \gg g z_m^2$ for $0 \le z \le z_m$ and $v_{max}(z_b - z_m) \gg D(z)$ or $g(z_b - z_m)^2 \gg D(z)$ for $z_m < z \le z_b$). The ESS distribution is convergence stable (Klausmeier and Litchman, 2001), and through either movement or growth the full model will converge on the simplified model when our inequalities for the deep layer hold.

If the mixed layer is well-mixed according to our inequalities, our simplified model approximates the full model well. If there is no mixed layer, then we have potential conditions for a surface bloom (see Model predictions in next section of discussion), essentially a completely poorly mixed water column ($z_m=0$). In between these two scenarios, the simplified model may not do a good job of approximating the full model.

Many phytoplankton groups such as cryptophytes, dinoflagellates, green algae, and chrysophytes have flagella and are actively motile. Other phytoplankton groups such as cyanobacteria and

even diatoms regulate their depth through physiological control of their buoyancy (Walsby, 1994; Cullen and MacIntyre, 1998; Waite et al., 1997). Our model applies broadly to all of these groups of phytoplankton.

However, not all phytoplankton can taxis along the gradient in growth rate because their taxis speed is too slow or mixing is too great. Some diatoms are well-mixed in the surface layer so $D(z) \gg v_{\max} z_m$ and $D(z) \gg g z_m^2$ for $0 \le z \le z_m$ and it would seem our model would hold under these conditions. However, criteria for the deep layer must also be met so that $v_{\max}(z_b - z_m) \gg D(z)$ or $g(z_b - z_m)^2 \gg D(z)$ for $z_m < z \le z_b$. Some diatoms and other species may not meet these criteria in the deep layer if mixing there is strong (large $D(z)$) or the water column is shallow (small $z_b - z_m$).

Deep water columns allow another way for even neutrally buoyant species to attain the ESS distribution by making it easier to satisfy the second condition for our approximation, $g(z_b - z_m)^2 \gg D(z)$. In this case, our model also does a reasonable job of approximating positively or negatively buoyant species with low but realistic speeds. However, our simplified model can deviate significantly from the full model (results not shown) for positively or negatively buoyant species with faster speeds ($> 0.2\,\mathrm{m\,d^{-1}}$) or in shallower water columns (such as 20 m). Buoyancy does not affect our results if z_e is in a perfectly mixed surface layer. Finally, sinking does not affect our results in the case of a benthic layer.

The assumption of a well-mixed layer can be broken in several ways. If $D(z)$ for $0 \le z \le z_m$ is small, then the mixed layer may not be considered well-mixed. If z_m is large, then this allows another way for the mixed layer to not be completely mixed, particularly if $v_{\max}$ is large or for species that are significantly positively or negatively buoyant. For example, in the case of $D(z) = 100\,\mathrm{m^2\,d^{-1}}$ for $0 \le z \le z_m$, a $z_m = 4$ m, and a positively buoyant species with velocities of $6\,\mathrm{m\,d^{-1}}$, the inequality where our simplified model approximates the full model breaks down and not only can there be non-uniform biomass in the mixed layer but addition of the high buoyancy can make the phytoplankton switch vertical distribution states completely in comparison to the state of a neutrally buoyant species.

The main cases our simplified model will not apply are when the mixed layer is intermediate between well- and poorly mixed and when the deep layer thickness ($z_b - z_m$) is small and phytoplankton cannot regulate their depth. These cases will require numerical solution of the full model, possibly with the addition of sinking or buoyancy (as in Huisman and Sommeijer, 2002a,b; Huisman et al., 2004; Jäger et al., 2010; Ryabov et al., 2010).

4.2. Model predictions

Increasing sediment nutrient concentration, R_{sed}, decreases the DCM depth and increases all biomass until it becomes light-limited (Fig. 4A). This prediction is in accordance with the trophic status hypothesis of Moll and Stoermer (1982) that nutrient-rich lakes will support a larger, shallower DCM. If we consider R_{sed} to be representative of trophic status, a comparison of the DCMs in relatively nutrient-rich Lake Michigan and nutrient-poor Lake Superior supports both our predictions and the trophic status hypothesis (Moll and Stoermer, 1982).

Increasing mixed layer nutrient input, R_{inML}, decreases DCM depth and increases mixed layer biomass, while having little effect on deep layer biomass (Fig. 4B). In Sawtooth Valley, Idaho lakes, experiments and simulations showed that fertilization in the form of surface nutrient input increases mixed layer biomass but had little effect on DCM biomass (Gross et al., 1997). Additionally, in Lake Geneva, a reduction in phosphorus inputs to the surface due to human activity has led to a deepening of the depth of DCM and annual nutrient depleted zone (Anneville and Leboulanger, 2001). Both of these studies support our predictions, contrary to other models which predict a tradeoff between mixed layer and deep layer biomass (Christensen et al., 1995).

Increasing background light attenuation, a_{bg}, generally decreases DCM depth and total biomass, especially the mixed layer biomass (Fig. 4C). Unfortunately, few empirical studies examine how background attenuation is related to vertical distribution and biomass, rather using total attenuation as the light-related environmental parameter. Total attenuation does, however, predict how the depth of the DCM varies both among and within the five Laurentian Great Lakes (Barbiero and Tuchman, 2001). In a comparison of two Finnish lakes, the dark water lake with high color values and shallow Secchi depth had a shallower depth distribution of phytoplankton than the clear water lake with low color values and deep Secchi depth (Holopainen et al., 2003). The negative effect of a_{bg} on mixed layer biomass is supported by experimental manipulation of background light attenuation in field enclosures (Diehl et al., 2002).

Mixed layer depth, z_m, can have a negative, positive, or no effect on biomass over some range of mixing depths dependent on the resource limitation state and vertical distribution of the phytoplankton (Fig. 4D). Less physically realistic models predict a unimodal relationship of mixed layer biomass with mixed layer depth (Huisman and Weissing, 1995; Diehl, 2002). Unfortunately, direct comparison of predictions from these other models with ours is hampered by additional processes such as nutrient input (Huisman and Weissing, 1995) and sinking (Diehl, 2002) that are directly proportional to mixed layer depth in their models.

While many environmental parameters vary widely between bodies of water, mixed layer depth also exhibits large variation seasonally within a body of water. Seasonal variation in mixed layer depth plays a major role in determining the seasonal cycle in vertical distribution and can affect the importance of deep layer biomass (Lindholm, 1992). Surprisingly, few studies have systematically examined effects of mixed layer depth on phytoplankton spatial and physiological structure. Mixed layer biomass showed a unimodal relationship with mixed layer depth across lakes (Kunz and Diehl, 2003) and within field enclosures (Diehl et al., 2002) which agrees with our prediction of state-dependent effects of z_m on B_{ML} (Fig. 4D). Both of these studies also support our prediction of a shift from nutrient limitation to light limitation with increasing mixed layer depth.

We also predict the depth of the DCM to be at the transition from nutrient limitation to light limitation, which is supported by data from Lake Tahoe (Coon et al., 1987). With increased nutrient input, biomass can reach very high levels in a light-limited mixed layer. Surface blooms often contain the most biomass throughout the season in a lake, which may support our prediction that decreasing z_m to zero in water columns with high nutrient levels can create extremely high biomass surface layers (Paerl, 1988).

4.3. Relevance

The fundamental relationships of phytoplankton with nutrients, light, and mixing revealed in our study may also guide lake management solutions. For example, in management of nutrient loading, not only the concentrations, but also the depths of input to the water column are important. Overall, the best way to reduce algal biomass is probably to reduce all nutrient inputs (R_{sed}, R_{inML}), but reducing inputs to the mixed layer (R_{inML}) may be the most effective for decreasing biomass, given our results. Some hypereutrophic lakes may require very large reductions in

phosphorus loading which may or may not help depending on the severity of phosphorus limitation for the phytoplankton as well as the potential for sediment phosphorus release (Marsden, 1989). If this is the situation, artificial mixing that increases mixing depth (z_m) may be the best option (Lorenzen and Mitchell, 1973; Visser et al., 1996), which is predicted to reduce biomass if it enhances light limitation (see also Huisman, 1999; Huisman et al., 1999; Diehl, 2002; Diehl et al., 2002).

Climate change affects the heat budget and other physical processes of a lake which, in turn, determine stratification and mixed layer depth. In particular, climate change may affect mixed layer depth (Magnuson et al., 1997; Schindler, 1997), which we predict to have state-dependent effects on phytoplankton vertical distribution and biomass (see Fig. 4D). Climate change also alters precipitation, hence the hydrological regime on the surrounding landscape that affects nutrient inputs and water clarity. Anthropogenically driven atmospheric nutrient deposition is also increasing, even in pristine areas (Hartmann et al., 2008; Neff et al., 2008). Climate induced changes in stratification and nutrient budgets have already affected phytoplankton community biomass and composition (Walsby et al., 1997; O'Reilly et al., 2003; Verburg et al., 2003; Jöhnk et al., 2008; Paerl and Huisman, 2009). An important task is to dissect how climate and other anthropogenically induced changes will be channeled through a number of environmental drivers to determine phytoplankton vertical distribution and production (Karlsson et al., 2009). Our model provides a spatially explicit framework to explore how multiple feedback loops between biotic and abiotic factors in the aquatic ecosystem will respond to human-induced environmental change.

Acknowledgements

Comments from Jim Grover, and several anonymous reviewers greatly improved this manuscript. This work was supported by funding from National Science Foundation Division of Environmental Biology 06-10531 and 06-10532 and the J.S. McDonnell Foundation. K.Y. was partially supported by the Global Environmental Research Fund (Fa-084) by the Ministry of the Environment, Japan. This is contribution number 1575 of the Kellogg Biological Station.

Appendix A

A.1. Derivation of equilibrium

Here we analyze stable steady states of our simplified model. At steady state, net growth is 0 in layers with positive biomass (Eq. (13)). Nutrients are constant in the surface layer ($R(z)\equiv\overline{R}_{ML}$ for $0\le z\le z_m$), and are linear with depth wherever there is no biomass in the deep layer ($d^2R/dz^2=0$ for $z_m<z<z_b$ where $b(z)=0$). For convenience, we specify vertical diffusion coefficient in the deep layer as D_{DL}.

At steady state, net nutrient flux equals net nutrient consumption by phytoplankton. In the surface layer, we have

$$-\frac{\overline{g}_{ML}B_{ML}}{Y}+\frac{\varepsilon mB_{ML}}{Y}+R_{inML}+D_{DL}\left.\frac{dR}{dz}\right|_{z=z_m^+}=0. \tag{A.1}$$

The first two terms of the left-hand side of Eq. (A.1) represent consumed and recycled nutrients within the surface layer, and the third and fourth terms, direct nutrient input to the surface layer and nutrient flux from the deep layer, respectively. Because $\overline{g}_{ML}-m=0$ when $B_{ML}>0$, Eq. (A.1) can be modified to

$$-\frac{m(1-\varepsilon)B_{ML}}{Y}+R_{inML}+D_{DL}\left.\frac{dR}{dz}\right|_{z=z_m^+}=0. \tag{A.2}$$

Note that Eq. (A.2) also holds when $B_{ML}=0$. Nutrient flux from the deep layer depends on whether biomass is present in the deep layer ($B_{DL}>0$) or not ($B_{DL}=0$). When $B_{DL}=0$, dR/dz is constant in the deep layer:

$$\frac{dR}{dz}=\frac{R(z_b)-\overline{R}_{ML}}{z_b-z_m}. \tag{A.3}$$

From the boundary condition at $z=z_b$ (5) and Eq. (A.3) we have

$$\frac{R(z_b)-\overline{R}_{ML}}{z_b-z_m}=h(R_{sed}-R(z_b)). \tag{A.4}$$

Rearranging Eq. (A.4), we obtain $R(z_b)$, and substituting $R(z_b)$ in Eq. (A.3), dR/dz is expressed by

$$\frac{dR}{dz}=\frac{R_{sed}-\overline{R}_{ML}}{z_b+1/h-z_m}. \tag{A.5}$$

According to Klausmeier and Litchman (2001), a stable DCM should be co-limited by nutrients and light (i.e., $R(z^*)=R^*$ and $I(z^{*+})=I^*$), and a stable benthic layer should be limited by nutrients (i.e., $R(z_b)=R^*$ and $I(z_b^+)\ge I^*$). Therefore, when $B_{DL}>0$, $R(z^*)=R^*$, and dR/dz is expressed by

$$\left.\frac{dR}{dz}\right|_{z=z_m^+}=\frac{R^*-\overline{R}_{ML}}{z^*-z_m}. \tag{A.6}$$

Substituting dR/dz in Eq. (A.2) with Eqs. (A.5) and (A.6), we have equalities for nutrient balance in the surface layer:

$$\begin{cases}-\dfrac{m(1-\varepsilon)B_{ML}}{Y}+R_{inML}+\dfrac{D_{DL}(R_{sed}-\overline{R}_{ML})}{z_b+1/h-z_m}=0 & \text{when } B_{DL}=0,\\ -\dfrac{m(1-\varepsilon)B_{ML}}{Y}+R_{inML}+\dfrac{D_{DL}(R^*-\overline{R}_{ML})}{z^*-z_m}=0 & \text{when } B_{DL}>0.\end{cases} \tag{A.7}$$

Similarly in the deep layer, we have an equality for nutrient balance at a depth with positive biomass z^*. When $z_m<z^*<z_b$ (DCM), we have

$$-\frac{m(1-\varepsilon)B_{DL}}{Y}+D_{DL}\left.\frac{dR}{dz}\right|_{z=z^{*+}}-D_{DL}\left.\frac{dR}{dz}\right|_{z=z^{*-}}=0. \tag{A.8}$$

The second and third terms of left-hand side of Eq. (A.8), respectively, denote nutrient fluxes from below and above z^*. Because $R(z^*)=R^*$ (Klausmeier and Litchman, 2001), these fluxes can be expressed by

$$D_{DL}\left.\frac{dR}{dz}\right|_{z=z^{*+}}=\frac{D_{DL}(R_{sed}-R^*)}{z_b+1/h-z^*},\quad D_{DL}\left.\frac{dR}{dz}\right|_{z=z^{*-}}=\frac{D_{DL}(R^*-\overline{R}_{ML})}{z^*-z_m}. \tag{A.9}$$

Substituting the fluxes in Eq. (A.8) with Eq. (A.9) we have an equality for nutrient balance at depth z^*,

$$-\frac{m(1-\varepsilon)B_{DL}}{Y}+\frac{D_{DL}(R_{sed}-R^*)}{z_b+1/h-z^*}-\frac{D_{DL}(R^*-\overline{R}_{ML})}{z^*-z_m}=0. \tag{A.10}$$

When $z^*=z_b$ (benthic layer), net nutrient flux is the sum of nutrient fluxes at sediment–water interface $[hD_{DL}(R_{sed}-R(z_b))=hD_{DL}(R_{sed}-R^*)]$ and from above z_b. Thus nutrient balance at benthic layer is written as

$$-\frac{m(1-\varepsilon)B_{DL}}{Y}+hD_{DL}(R_{sed}-R^*)-\frac{D_{DL}(R^*-\overline{R}_{ML})}{z_b-z_m}=0. \tag{A.11}$$

We can see that Eq. (A.10) implies Eq. (A.11) when $z^*=z_b$. Therefore the equality (Eq. (A.10)) holds for $z_m<z^*\le z_b$, which expresses nutrient balance at either a DCM or a benthic layer.

The light profile is expressed by

$$I(z)=\begin{cases} I_{\mathrm{in}}e^{-(a_{\mathrm{bg}}z+aB_{\mathrm{ML}}z/z_{\mathrm{m}})} & \text{for } 0\le z\le z_{\mathrm{m}},\\ I_{\mathrm{in}}e^{-(a_{\mathrm{bg}}z+aB_{\mathrm{ML}})} & \text{for } z_{\mathrm{m}}<z<z^{*},\\ I_{\mathrm{in}}e^{-(a_{\mathrm{bg}}z+aB_{\mathrm{ML}}+aB_{\mathrm{DL}})} & \text{for } z^{*}\le z\le z_{\mathrm{b}}. \end{cases} \tag{A.12}$$

Steady state distributions are obtained by solving equations for zero net growth (Eq. (13)), nutrient balance in the surface layer (Eq. (A.7)), and nutrient balance in the deep layer (Eq. (A.10)), with the light profile (Eq. (A.12)). We always found a unique steady state for a given set of parameters. Conditions (14) should be satisfied for a steady state distribution to be an ESS.

In the following, we first write down $\overline{g}_{\mathrm{ML}}$ when growth in the surface layer is limited by light, limited by nutrients, or co-limited by nutrients and light for later convenience. Next we show that four cases out of the 12 logically possible combinations of biomass in the mixed and deep layers are theoretically infeasible, leaving eight possible cases. Then we solve for the steady states of these cases, and evaluate their stability.

A.2. Growth in the surface layer

In the following, we first write down $\overline{g}_{\mathrm{ML}}$ when growth in the surface layer is limited by light, limited by nutrients, or co-limited by nutrients and light for later convenience. Next we show that four cases out of the 12 logically possible combinations of biomass in the mixed and deep layers are theoretically infeasible, leaving eight possible cases. Then we solve for the steady states of these cases, and evaluate their stability.

Growth in the surface layer $\overline{g}_{\mathrm{ML}}$ is written as

$$\overline{g}_{\mathrm{ML}}=\frac{1}{z_{\mathrm{m}}}\int_0^{z_{\mathrm{m}}}\min(f_I(I(z)),f_R(\overline{R}_{\mathrm{ML}}))\,dz. \tag{A.13}$$

When $f_R(\overline{R}_{\mathrm{ML}})\ge f_I(I_{\mathrm{in}})$, growth is limited by light only, and $\overline{g}_{\mathrm{ML}}$ is

$$\overline{g}_{\mathrm{ML}}=\frac{1}{z_{\mathrm{m}}}\int_0^{z_{\mathrm{m}}}f_I(I(z))\,dz. \tag{A.14}$$

When we use a Michaelis–Menten formulation $f_I(I)=rI/(I+K_I)$, the integral can be computed following Monsi and Saeki (1953) and Huisman and Weissing (1994):

$$\overline{g}_{\mathrm{ML}}=\frac{r}{a_{\mathrm{bg}}z_{\mathrm{m}}+aB_{\mathrm{ML}}}\log\left[\frac{K_I+I_{\mathrm{in}}}{K_I+I_{\mathrm{in}}e^{-(a_{\mathrm{bg}}z_{\mathrm{m}}+aB_{\mathrm{ML}})}}\right]. \tag{A.15}$$

When $f_R(\overline{R}_{\mathrm{ML}})\le f_I(I(z_{\mathrm{m}}))$, growth is limited by nutrients only, and the integral is trivially computed:

$$\overline{g}_{\mathrm{ML}}=f_R(\overline{R}_{\mathrm{ML}}). \tag{A.16}$$

When $f_I(I(z_{\mathrm{m}}))<f_R(\overline{R}_{\mathrm{ML}})<f_I(I_{\mathrm{in}})$, growth is co-limited by nutrients and light. Because $f_I(I(z))-f_R(\overline{R}_{\mathrm{ML}})$ decreases monotonically for $0\le z\le z_{\mathrm{m}}$, there is a unique co-limitation depth $0\le z_{\mathrm{e}}\le z_{\mathrm{m}}$ that satisfies

$$f_R(\overline{R}_{\mathrm{ML}})=f_I(I(z_{\mathrm{e}})), \tag{A.17}$$

and the integral splits into a nutrient-limited and a light-limited part:

$$\overline{g}_{\mathrm{ML}}=\frac{1}{z_{\mathrm{m}}}\left[\int_0^{z_{\mathrm{e}}}f_R(\overline{R}_{\mathrm{ML}})\,dz+\int_{z_{\mathrm{e}}}^{z_{\mathrm{m}}}f_I(I(z))\,dz\right]. \tag{A.18}$$

Each integral of Eq. (A.18) is computed following Eqs. (A.15) and (A.16):

$$\overline{g}_{\mathrm{ML}}=\frac{z_{\mathrm{e}}}{z_{\mathrm{m}}}f_R(\overline{R}_{\mathrm{ML}})+\frac{r}{a_{\mathrm{bg}}z_{\mathrm{m}}+aB_{\mathrm{ML}}}\log\left[\frac{K_I+I_{\mathrm{in}}e^{-(a_{\mathrm{bg}}z_{\mathrm{e}}+aB_{\mathrm{ML}}z_{\mathrm{e}}/z_{\mathrm{m}})}}{K_I+I_{\mathrm{in}}e^{-(a_{\mathrm{bg}}z_{\mathrm{m}}+aB_{\mathrm{ML}})}}\right]. \tag{A.19}$$

To summarize, $\overline{g}_{\mathrm{ML}}$ is expressed by Eq. (A.15) when $f_R(\overline{R}_{\mathrm{ML}})\ge f_I(I_{\mathrm{in}})$, by Eq. (A.16) when $f_R(\overline{R}_{\mathrm{ML}})\le f_I(I_{\mathrm{in}})$, and by Eq. (A.19) when $f_I(I(z_{\mathrm{m}}))<f_R(\overline{R}_{\mathrm{ML}})<f_I(I_{\mathrm{in}})$. The co-limitation depth z_{e} is obtained from Eq. (A.17).

A.3. Four infeasible cases

Under light limitation, $\partial g/\partial I=df_I/dI>0$ while g is independent of nutrients ($\partial g/\partial R=0$) from our assumption. Light decreases with depth $dI/dz<0$, and nutrients are constant in the surface layer $dR/dz=0$. Differentiating g with respect to z we have

$$\frac{dg}{dz}=\frac{\partial g}{\partial I}\frac{dI}{dz}+\frac{\partial g}{\partial R}\frac{dR}{dz}. \tag{A.20}$$

Thus $dg/dz<0$ under light limitation. Likewise, $dg/dz=0$ under nutrient limitation in the surface layer. As we saw before, there is a unique co-limitation depth z_{e} when growth is co-limited by nutrients and light in the surface layer, and below z_{e}, growth is limited by light. Therefore the following inequality is satisfied under co-limitation or light limitation:

$$g(z)>g(z_{\mathrm{m}})\quad\text{for } 0\le z<z_{\mathrm{m}}. \tag{A.21}$$

Suppose there is positive biomass in the surface layer, $B_{\mathrm{ML}}>0$, whose growth is limited by light or co-limited by nutrients and light, and $g(z_{\mathrm{m}})-m\ge 0$. Because of Eq. (A.21) it is obvious that net growth in the surface layer satisfies

$$\frac{1}{z_{\mathrm{m}}}\int_0^{z_{\mathrm{m}}}(g(z)-m)\,dz>0. \tag{A.22}$$

This contradicts the first equality of Eq. (13). Therefore $g(z_{\mathrm{m}})-m<0$ when $B_{\mathrm{ML}}>0$ and the growth is limited by light or co-limited. Because $g(z_{\mathrm{m}})-m<0$, $I(z_{\mathrm{m}})<I^{*}$. Therefore $g(z)-m<0$ for $z_{\mathrm{m}}<z\le z_{\mathrm{b}}$. This prevents the second equality of Eq. (13) from being satisfied anywhere in the deep layer, and hence B_{DL} should be 0.

To conclude, if $B_{\mathrm{ML}}>0$ and the growth is limited by light or co-limited by nutrients and light, $B_{\mathrm{DL}}=0$ at steady state. This excludes four cases, (DCM)+(light-limited ML), (DCM)+(co-limited ML), (benthic layer)+(co-limited ML), and (benthic layer)+(light-limited ML), from steady state distributions.

A.4. Eight possible cases

Case 1: *Empty*.
Knowns: $B_{\mathrm{ML}}=0$, $B_{\mathrm{DL}}=0$.
Unknowns: $\overline{R}_{\mathrm{ML}}$.
Equations to solve: Because $B_{\mathrm{ML}}=B_{\mathrm{DL}}=0$, we have only one equation derived from Eq. (A.7) to solve for one unknown $\overline{R}_{\mathrm{ML}}$:

$$R_{\mathrm{inML}}+\frac{D_{\mathrm{DL}}(R_{\mathrm{sed}}-\overline{R}_{\mathrm{ML}})}{z_{\mathrm{b}}+1/h-z_{\mathrm{m}}}=0, \tag{A.23}$$

and obtain

$$\overline{R}_{\mathrm{ML}}=R_{\mathrm{sed}}+\frac{(z_{\mathrm{b}}+1/h-z_{\mathrm{m}})R_{\mathrm{inML}}}{D_{\mathrm{DL}}}. \tag{A.24}$$

From Eq. (A.12) light profile is expressed by

$$I(z)=I_{\mathrm{in}}e^{-a_{\mathrm{bg}}z}. \tag{A.25}$$

Consistency/stability criteria: It is easy to see that $\overline{g}_{\mathrm{ML}}\ge g(z)$ for $z_{\mathrm{m}}<z\le z_{\mathrm{b}}$. Therefore the case "empty" is stable when $\overline{g}_{\mathrm{ML}}-m\le 0$. From Eqs. (A.15), (A.16), and (A.19), this condition is summarized by

$$\begin{cases} \dfrac{r}{a_{\mathrm{bg}}z_{\mathrm{m}}}\log\left(\dfrac{K_I+I_{\mathrm{in}}}{K_I+I_{\mathrm{in}}e^{-a_{\mathrm{bg}}z_{\mathrm{m}}}}\right)-m\le 0 & \text{when } f_R(\overline{R}_{\mathrm{ML}})\ge f_I(I_{\mathrm{in}}),\\ \dfrac{z_{\mathrm{e}}}{z_{\mathrm{m}}}f_R(\overline{R}_{\mathrm{ML}})+\dfrac{r}{a_{\mathrm{bg}}z_{\mathrm{m}}}\log\left(\dfrac{K_I+I_{\mathrm{in}}}{K_I+I_{\mathrm{in}}e^{-a_{\mathrm{bg}}z_{\mathrm{m}}}}\right)-m\le 0 & \text{when } f_I(I(z_{\mathrm{m}}))<f_R(\overline{R}_{\mathrm{ML}})<f_I(I_{\mathrm{in}}),\\ f_R(\overline{R}_{\mathrm{ML}})-m\le 0 & \text{when } f_R(\overline{R}_{\mathrm{ML}})\le f_I(I(z_{\mathrm{m}})), \end{cases} \tag{A.26}$$

where z_e is obtained from Eq. (A.17). The frontier of the first inequality of Eq. (A.26),

$$\frac{r}{a_{bg}z_m}\log\left(\frac{K_I+I_{in}}{K_I+I_{in}e^{-a_{bg}z_m}}\right)-m=0, \tag{A.27}$$

separates empty and light-limited ML regions; the second,

$$\frac{z_e}{z_m}f_R(\overline{R}_{ML})+\frac{r}{a_{bg}z_m}\log\left(\frac{K_I+I_{in}e^{-a_{bg}z_e}}{K_I+I_{in}e^{-a_{bg}z_m}}\right)-m=0, \tag{A.28}$$

separates empty and co-limited ML regions. The third inequality of Eq. (A.26) implies $\overline{R}_{ML}\le R^*$ and the frontier,

$$R_{sed}+\frac{(z_b+1/h-z_m)R_{inML}}{D_{DL}}=R^*, \tag{A.29}$$

separates the empty and the benthic layer or DCM or nutrient-limited ML or some possible combination of these cases.

Case 2: *Co-limited mixed layer*.

Knowns: $B_{DL}=0$.

Unknowns: B_{ML}, z_e, $\overline{R}_{ML}$.

Equations to solve: Because $B_{ML}>0$ and $B_{DL}=0$ we have equalities from Eqs. (13) and (A.7) to solve for $\overline{R}_{ML}$ and B_{ML}:

$$-\frac{m(1-\varepsilon)B_{ML}}{Y}+R_{inML}+\frac{D_{DL}(R_{sed}-\overline{R}_{ML})}{z_b+1/h-z_m}=0, \tag{A.30}$$

$$(\overline{g}_{ML}-m=)\frac{1}{z_m}\left[\int_0^{z_m}\min(f_I(I(z)),f_R(\overline{R}_{ML}))\,dz\right]-m=0, \tag{A.31}$$

where the light profile is from Eq. (A.12):

$$I(z)=\begin{cases} I_{in}e^{-(a_{bg}z+aB_{ML}z/z_m)} & \text{for } 0\le z\le z_m,\\ I_{in}e^{-(a_{bg}z+aB_{ML})} & \text{for } z_m<z\le z_b.\end{cases} \tag{A.32}$$

Specifically when growth is co-limited by nutrients and light, $\overline{g}_{ML}$ is expressed by Eq. (A.19), and the equality equation (A.31) is rewritten by

$$\frac{z_e}{z_m}f_R(\overline{R}_{ML})+\frac{r}{a_{bg}z_m+aB_{ML}}\log\left[\frac{K_I+I_{in}e^{-(a_{bg}z_e+aB_{ML}z_e/z_m)}}{K_I+I_{in}e^{-(a_{bg}z_m+aB_{ML})}}\right]-m=0, \tag{A.33}$$

where z_e is obtained from Eq. (A.17). Eqs. (A.30) and (A.33) are solved numerically for unknowns B_{ML} and $\overline{R}_{ML}$ with z_e from Eq. (A.17).

Consistency/stability criteria: Stability is already ensured because $I(z)<I(z_m)<I^*$ for $z_m<z\le z_b$ (see "Four impossible cases" section for the proof). Existence of positive steady state requires positive biomass $B_{ML}>0$ and equal limitation depth within the surface layer $0<z_e<z_m$. The frontier of the first inequality is obtained by setting $B_{ML}=0$ in Eqs. (A.30), (A.33), and (A.17), which is identical to the second inequality of Eq. (A.28). This separates co-limited ML and empty regions. One frontier of the second inequality is obtained by setting $z_e=0$ in Eqs. (A.30), (A.33), and (A.17):

$$\begin{cases} -\dfrac{m(1-\varepsilon)B_{ML}}{Y}+R_{inML}+\dfrac{D_{DL}(R_{sed}-\overline{R}_{ML})}{z_b+1/h-z_m}=0,\\ \dfrac{r}{a_{bg}z_m+aB_{ML}}\log\left[\dfrac{K_I+I_{in}}{K_I+I_{in}e^{-(a_{bg}z_m+aB_{ML})}}\right]-m=0,\\ f_I(I_{in})-f_R(\overline{R}_{ML})=0.\end{cases} \tag{A.34}$$

When we use Michaelis–Menten formulations for f_I and f_R, we obtain an equality algebraically from Eq. (A.34). This frontier separates co-limited and light-limited ML regions. The other one is obtained by setting $z_e=z_m$ in Eqs. (A.30), (A.33), and (A.17):

$$\begin{cases} -\dfrac{m(1-\varepsilon)B_{ML}}{Y}+R_{inML}+\dfrac{D_{DL}(R_{sed}-\overline{R}_{ML})}{z_b+1/h-z_m}=0,\\ f_R(\overline{R}_{ML})-m=0,\\ f_I(I_{in}e^{-(a_{bg}z_m+aB_{ML})})-f_R(\overline{R}_{ML})=0.\end{cases} \tag{A.35}$$

From the second equality of Eq. (A.35), $\overline{R}_{ML}=R^*$. From the second and the third equalities, we have

$$I_{in}e^{-(a_{bg}z_m+aB_{ML})}=I^*, \tag{A.36}$$

which yields

$$B_{ML}=\frac{\log(I_{in}/I^*)-a_{bg}z_m}{a}. \tag{A.37}$$

Substituting $\overline{R}_{ML}=R^*$ and Eq. (A.37) in the first equality of Eq. (A.35) we obtain

$$\frac{YD_{DL}(R_{sed}-R^*)}{m(1-\varepsilon)(z_b+1/h-z_m)}-\frac{\log(I_{in}/I^*)-a_{bg}z_m}{a}+\frac{YR_{inML}}{m(1-\varepsilon)}=0. \tag{A.38}$$

When $R_{inML}=0$, Eq. (A.38) is identical with Eq. (A.74), and separates co-limited ML and DCM regions.

Case 3: *Light-limited mixed layer*.

Knowns: $B_{DL}=0$.

Unknowns: B_{ML}, $\overline{R}_{ML}$.

Equations to solve. $B_{ML}>0$ and $B_{DL}=0$ in this case, thus the same equalities (Eqs. (A.30) and (A.31)) with the light profile (Eq. (A.32)) hold as in the co-limited ML case. Under light limitation for growth, $\overline{g}_{ML}$ is expressed by Eqs. (A.15) and (A.31) is rewritten by

$$\frac{r}{a_{bg}z_m+aB_{ML}}\log\left[\frac{K_I+I_{in}}{K_I+I_{in}e^{-(a_{bg}z_m+aB_{ML})}}\right]-m=0. \tag{A.39}$$

Equalities (Eqs. (A.30) and (A.39)) are solved numerically for the two unknowns $\overline{R}_{ML}$ and B_{ML}.

Consistency/stability criteria: Stability is ensured because $I(z)<I(z_m)<I^*$ for $z_m<z\le z_b$. The existence of a positive steady state requires $B_{ML}>0$ and $f_I(I_{in})<f_R(\overline{R}_{ML})$. The frontier of the first inequality is obtained by setting $B_{ML}=0$ in Eqs. (A.30) and (A.39), which is identical with Eq. (A.27). The frontier of the second inequality is obtained by setting $f_I(I_{in})-f_R(\overline{R}_{ML})=0$, which is identical with what is obtained from Eq. (A.34).

Case 4: *Nutrient-limited mixed layer*.

Knowns: $B_{DL}=0$, $\overline{R}_{ML}=R^*$.

Unknowns: B_{ML}.

Equations to solve: The same equalities (Eqs. (A.30) and (A.31)) with light profile (Eq. (A.32)) hold because $B_{ML}>0$ and $B_{DL}=0$ in this case. Under nutrient limitation for growth, $\overline{g}_{ML}$ is expressed by Eqs. (A.16) and (A.31) is,

$$f_R(\overline{R}_{ML})-m=0, \tag{A.40}$$

which means $\overline{R}_{ML}=R^*$. Substituting $\overline{R}_{ML}=R^*$ in Eq. (A.30), we obtain

$$-\frac{m(1-\varepsilon)B_{ML}}{Y}+R_{inML}+\frac{D_{DL}(R_{sed}-R^*)}{z_b+1/h-z_m}=0. \tag{A.41}$$

Rearranging Eq. (A.41) we have B_{ML}:

$$B_{ML}=\frac{YR_{inML}}{m(1-\varepsilon)}+\frac{YD_{DL}(R_{sed}-R^*)}{m(1-\varepsilon)(z_b+1/h-z_m)}. \tag{A.42}$$

Consistency/stability criteria: The existence of a positive steady state requires $B_{ML}>0$ and $f_I(I(z_m))>f(\overline{R}_{ML})$ $(=m)$. The latter inequality implies $I(z_m)>I^*$. The frontier of the first inequality is obtained from Eq. (A.42), which is identical with Eq. (A.29). The frontier of the second inequality is rewritten as

$$I_{in}e^{-(a_{bg}z_m+aB_{ML})}=I^*. \tag{A.43}$$

Substituting B_{ML} with Eq. (A.42) in Eq. (A.43), some rearrangement gives the same equality as Eq. (A.38).

Stability requires $g(z)-m \le 0$ for $z_m < z \le z_b$. When $B_{DL}=0$ and $R_{sed} > \overline{R}_{ML}$, $dR/dz > 0$ from Eq. (A.5). Because $\overline{R}_{ML} = R^*$ here, we have $R(z) > R^*$ for $z_m < z \le z_b$ in this case. With $I(z_m) > I^*$, there is $\delta > 0$ such that $g(z_m+\delta)-m > 0$. Therefore a nutrient-limited ML is unstable when $R_{sed} > R^*$ and is stable when $R_{sed} \le R^*$. Considering the conditions for existence $B_{ML} > 0$ and stability $R_{sed} \le R^*$, some rearrangement of Eq. (A.42) gives an inequality $R_{inML} > 0$ that must be satisfied.

Case 5: *Benthic layer and nutrient-limited mixed layer.*

Knowns: $\overline{R}_{ML} = R^*$.

Unknowns: B_{ML}, B_{DL}.

Equations to solve: Growth in the surface layer is limited by nutrients, that is, $\overline{R}_{ML} = R^*$. Because $B_{ML} > 0$, $B_{DL} > 0$, and $\overline{R}_{ML} = R^*$, we have equalities from Eqs. (A.7) and (A.10):

$$-\frac{m(1-\varepsilon)B_{ML}}{Y} + R_{inML} = 0, \tag{A.44}$$

$$-\frac{m(1-\varepsilon)B_{DL}}{Y} + hD_{DL}(R_{sed}-R^*) = 0, \tag{A.45}$$

and obtain,

$$B_{ML} = \frac{YR_{inML}}{m(1-\varepsilon)}, \tag{A.46}$$

$$B_{DL} = \frac{hYD_{DL}(R_{sed}-R^*)}{m(1-\varepsilon)}. \tag{A.47}$$

The light profile is expressed by Eq. (A.12).

Consistency/stability criteria: Stability is ensured because $R(z)=R^*$ for $0 \le z \le z_b$. The existence of a positive steady state requires $B_{ML} > 0$, $B_{DL} > 0$, and $I(z_b) \ge I^*$. These first two conditions imply $R_{inML} > 0$ and $R_{sed} > R^*$, respectively. The frontiers $R_{inML}=0$ separates (benthic layer + nutrient-limited ML) and benthic layer regions, and $R_{sed}=R^*$, (benthic layer + nutrient-limited ML) and nutrient-limited ML regions. Substituting B_{ML} and B_{DL} in Eq. (A.12) with Eqs. (A.46) and (A.47), the last condition $I(z_b) \ge I^*$ is rewritten as

$$I_{in}e^{-[a_{bg}z_b + aYR_{inML}/m(1-\varepsilon) + ahYD_{DL}(R_{sed}-R^*)/m(1-\varepsilon)]} \ge I^*, \tag{A.48}$$

which is rearranged to get

$$\frac{hYD_{DL}(R_{sed}-R^*)}{m(1-\varepsilon)} - \frac{\log(I_{in}/I^*)-a_{bg}z_b}{a} + \frac{YR_{inML}}{m(1-\varepsilon)} \le 0. \tag{A.49}$$

The frontier of Eq. (A.49) separates the (benthic layer + nutrient-limited ML) and (DCM + nutrient-limited ML) regions.

Case 6: *DCM and nutrient-limited mixed layer.*

Knowns: $\overline{R}_{ML} = R^*$.

Unknowns: B_{ML}, B_{DL}, z^*.

Equations to solve: Because $B_{ML} > 0$, $B_{DL} > 0$, and $\overline{R}_{ML} = R^*$, we obtain equalities (Eq. (A.44)) and

$$-\frac{m(1-\varepsilon)B_{DL}}{Y} + \frac{D_{DL}(R_{sed}-R^*)}{z_b+1/h-z^*} = 0, \tag{A.50}$$

from Eqs. (A.7) and (A.10). Light profile is expressed by Eq. (A.12). At z^*, growth is co-limited by nutrients and light, thus $I(z^{*+}) = I^*$:

$$I_{in}e^{-(a_{bg}z^* + aB_{ML} + aB_{DL})} = I^*. \tag{A.51}$$

From Eq. (A.44) we obtain B_{ML}, which is expressed by Eq. (A.46). Equalities equations (A.50) and (A.51) are simultaneously solved for B_{DL} and z^*.

Consistency/stability criteria: DCM and nutrient-limited ML is stable because $R(z)=R^*$ for $0 \le z < z^*$ and $I(z) \le I^*$ for $z^* \le z \le z_b$. The existence of a positive steady state requires: $B_{ML} > 0$, $B_{DL} > 0$, and $z_m < z^* < z_b$. The first condition is satisfied when $R_{inML} > 0$. Rearranging Eq. (A.50), we get

$$B_{DL} = \frac{YD_{DL}(R_{sed}-R^*)}{m(1-\varepsilon)(z_b+1/h-z^*)}. \tag{A.52}$$

Substituting B_{ML} from Eqs. (A.46), Eq. (A.51) is rearranged and we get

$$B_{DL} = \frac{\log(I_{in}/I^*)-a_{bg}z^*}{a} - \frac{YR_{inML}}{m(1-\varepsilon)}. \tag{A.53}$$

From Eqs. (A.52) and (A.53) we have an equality:

$$\frac{YD_{DL}(R_{sed}-R^*)}{m(1-\varepsilon)(z_b+1/h-z^*)} = \frac{\log(I_{in}/I^*)-a_{bg}z^*}{a} - \frac{YR_{inML}}{m(1-\varepsilon)}, \tag{A.54}$$

which is solved for z^*. The one frontier of the condition $z_m < z^* < z_b$ is obtained by substituting $z^*=z_m$ in Eq. (A.54):

$$\frac{YD_{DL}(R_{sed}-R^*)}{m(1-\varepsilon)(z_b+1/h-z_m)} - \frac{\log(I_{in}/I^*)-a_{bg}z_m}{a} + \frac{YR_{inML}}{m(1-\varepsilon)} = 0, \tag{A.55}$$

which is identical with Eq. (A.38) and separates (DCM + nutrient-limited ML) and co-limited ML regions. The other one is obtained by substituting $z^*=z_b$:

$$\frac{hYD_{DL}(R_{sed}-R^*)}{m(1-\varepsilon)} - \frac{\log(I_{in}/I^*)-a_{bg}z_b}{a} + \frac{YR_{inML}}{m(1-\varepsilon)} = 0, \tag{A.56}$$

which is identical with the frontier of Eq. (A.49), and separates the (DCM + nutrient-limited ML) and (benthic layer + nutrient-limited ML) regions.

Case 7: *Benthic layer* (*BL*).

Knowns: $B_{ML}=0$.

Unknowns: B_{DL}, $\overline{R}_{ML}$.

Equations to solve: When $B_{ML}=0$ and $z^*=z_b$, the following equalities are derived from Eqs. (A.7) and (A.10):

$$\begin{aligned} &R_{inML} + \frac{D_{DL}(R^*-\overline{R}_{ML})}{z_b-z_m} = 0, \\ &-\frac{m(1-\varepsilon)B_{DL}}{Y} + hD_{DL}(R_{sed}-R^*) - \frac{D_{DL}(R^*-\overline{R}_{ML})}{z_b-z_m} = 0, \end{aligned} \tag{A.57}$$

and we obtain two unknowns:

$$\overline{R}_{ML} = R^* + \frac{(z_b-z_m)R_{inML}}{D_{DL}}, \tag{A.58}$$

$$B_{DL} = \frac{hYD_{DL}(R_{sed}-R^*)}{m(1-\varepsilon)} + \frac{YR_{inML}}{m(1-\varepsilon)}. \tag{A.59}$$

From Eq. (A.12), the light profile is

$$I(z) = \begin{cases} I_{in}e^{-a_{bg}z} & \text{for } 0 \le z < z_b, \\ I_{in}e^{-(a_{bg}z + aB_{DL})} & \text{for } z = z_b. \end{cases} \tag{A.60}$$

Consistency/stability criteria: First we consider the existence of the positive steady state. From Eq. (A.59), $B_{DL} > 0$ when

$$hD_{DL}(R_{sed}-R^*) + R_{inML} > 0. \tag{A.61}$$

Net growth $g(z_b) - m = 0$ when

$$I(z_b) = I_{in}e^{-(a_{bg}z_b + aB_{DL})} \ge I^*. \tag{A.62}$$

The two above inequalities (Eqs. (A.61) and (A.62)) ensure the existence of a positive steady state.

Next we consider the stability criteria. Net growth should be negative or 0 everywhere for the stability. When $R_{inML}=0$, $g(z) - m = 0$ because $R(z)=R^*$ for $0 \le z \le z_b$, and hence benthic layer is stable. When $R_{inML} > 0$, the benthic layer is unstable because $\overline{R}_{ML} > R^*$ from (Eq. (A.58)) and $I(z) > I^*$ from (Eq. (A.62)).

To summarize, the stability of the benthic layer requires $R_{inML}=0$; in this case, the inequality (Eq. (A.61)) is simplified, and the parameter region where the deep layer is stable is

expressed by

$$\begin{cases} R_{\text{sed}} - R^* > 0, \\ I_{\text{in}} e^{-(a_{\text{bg}} z_{\text{b}} + a B_{\text{DL}})} \geq I^*. \end{cases} \tag{A.63}$$

The frontier of the first inequality, $R_{\text{sed}} = R^*$, separates the benthic layer and empty regions, which is identical with Eq. (A.29) when $R_{\text{inML}} = 0$. Substituting B_{DL} with Eq. (A.59), the frontier of the second inequality of Eq. (A.63) is written as

$$\frac{hYD_{\text{DL}}(R_{\text{sed}} - R^*)}{m(1-\varepsilon)} - \frac{\log(I_{\text{in}}/I^*) - a_{\text{bg}} z_{\text{b}}}{a} = 0, \tag{A.64}$$

which separates the benthic layer and DCM regions.

Case 8: *DCM*.

Knowns: $B_{\text{ML}} = 0$.

Unknowns: B_{DL}, z^*, $\overline{R}_{\text{ML}}$.

Equations to solve: When $B_{\text{ML}} = 0$, the following equalities are obtained from Eqs. (A.7) and (A.10):

$$R_{\text{inML}} + \frac{D_{\text{DL}}(R^* - \overline{R}_{\text{ML}})}{z^* - z_{\text{m}}} = 0, \tag{A.65}$$

$$-\frac{m(1-\varepsilon)B_{\text{DL}}}{Y} + \frac{D_{\text{DL}}(R_{\text{sed}} - R^*)}{z_{\text{b}} + 1/h - z^*} - \frac{D_{\text{DL}}(R^* - \overline{R}_{\text{ML}})}{z^* - z_{\text{m}}} = 0. \tag{A.66}$$

From Eq. (A.12), the light profile can be expressed by

$$I(z) = \begin{cases} I_{\text{in}} e^{-a_{\text{bg}} z} & \text{for } 0 \leq z < z^*, \\ I_{\text{in}} e^{-(a_{\text{bg}} z + a B_{\text{DL}})} & \text{for } z^* \leq z \leq z_{\text{b}}. \end{cases} \tag{A.67}$$

A stable DCM must be co-limited by nutrients and light. Therefore $I(z^{*+}) = I^*$, that is,

$$I_{\text{in}} e^{-(a_{\text{bg}} z^* + a B_{\text{DL}})} = I^*. \tag{A.68}$$

Solving Eqs. (A.65), (A.66), and (A.68), we obtain three unknowns, $\overline{R}_{\text{ML}}$, B_{DL}, and z^*.

Consistency/stability criteria: As with the case of a benthic layer, a DCM is unstable when $R_{\text{inML}} > 0$ because $\overline{R}_{\text{ML}} > R^*$ from Eq. (A.65) and $I(z) > I^*$ for $0 \leq z < z^*$ from Eq. (A.68). So we consider $R_{\text{inML}} = 0$. In this case, $\overline{R}_{\text{ML}} = R^*$, and rearranging Eq. (A.66) we have

$$B_{\text{DL}} = \frac{YD_{\text{DL}}(R_{\text{sed}} - R^*)}{m(1-\varepsilon)(z_{\text{b}} + 1/h - z^*)}, \tag{A.69}$$

and rearranging Eq. (A.68) we have

$$B_{\text{DL}} = \frac{\log(I_{\text{in}}/I^*) - a_{\text{bg}} z^*}{a}. \tag{A.70}$$

From Eqs. (A.69) and (A.70) an equality is obtained:

$$\frac{YD_{\text{DL}}(R_{\text{sed}} - R^*)}{m(1-\varepsilon)(z_{\text{b}} + 1/h - z^*)} = \frac{\log(I_{\text{in}}/I^*) - a_{\text{bg}} z^*}{a}, \tag{A.71}$$

which is solved algebraically for z^* (Klausmeier and Litchman, 2001). The obtained z^* should satisfy

$$z_{\text{m}} < z^* < z_{\text{b}}. \tag{A.72}$$

From Eq. (A.69), the existence of a positive steady state requires

$$R_{\text{sed}} > R^*. \tag{A.73}$$

$R_{\text{inML}} = 0$ and inequalities (Eqs. (A.72) and (A.73)) define the parameter region where the DCM is stable.

One frontier of Eq. (A.72), $z^* = z_{\text{m}}$, is expressed by substituting z^* in Eq. (A.71) with z_{m}:

$$\frac{YD_{\text{DL}}(R_{\text{sed}} - R^*)}{m(1-\varepsilon)(z_{\text{b}} + 1/h - z_{\text{m}})} - \frac{\log(I_{\text{in}}/I^*) - a_{\text{bg}} z_{\text{m}}}{a} = 0, \tag{A.74}$$

which separates DCM and co-limited ML regions, and the other one, $z^* = z_{\text{b}}$,

$$\frac{hYD_{\text{DL}}(R_{\text{sed}} - R^*)}{m(1-\varepsilon)} - \frac{\log(I_{\text{in}}/I^*) - a_{\text{bg}} z_{\text{b}}}{a} = 0, \tag{A.75}$$

separates the DCM and benthic layer regions. Note that this frontier is identical with Eq. (A.64). The frontier of Eq. (A.73), $R_{\text{sed}} = R^*$, separates the DCM and empty regions.

References

Anneville, O., Leboulanger, C., 2001. Long-term changes in the vertical distribution of phytoplankton biomass and primary production in Lake Geneva: a response to the oligotrophication. Alti Associazione Italiana Oceanologia Limnologia 14, 25–35.

Barbiero, R.P., Tuchman, M.L., 2001. Results from the US EPA's biological open water surveillance program of the Laurentian Great Lakes: II. Deep chlorophyll maxima. Journal of Great Lakes Research 27, 155–166.

Beckmann, A., Hense, I., 2007. Beneath the surface: characteristics of oceanic ecosystems under weak mixing conditions—a theoretical investigation. Progress in Oceanography 75, 771–796.

Brown, P.N., Byrne, G.D., Hindmarsh, A.C., 1989. VODE—a variable-coefficient ODE solver. SIAM Journal on Scientific & Statistical Computing 10, 1038–1051.

Camacho, A., 2006. On the occurrence and ecological features of deep chlorophyll maxima (DCM) in Spanish stratified lakes. Limnetica 25, 453–478.

Christensen, D.L., Carpenter, S.R., Cottingham, K.L., 1995. Predicting chlorophyll vertical-distribution in response to epilimnetic nutrient enrichment in small stratified lakes. Journal of Plankton Research 17, 1461–1477.

Condie, S.A., Bormans, M., 1997. The influence of density stratification on particle settling, dispersion and population growth. Journal of Theoretical Biology 187, 65–75.

Coon, T.G., Lopez, M., Richerson, P.J., Powell, T.M., Goldman, C.R., 1987. Summer dynamics of the deep chlorophyll maximum in Lake Tahoe. Journal of Plankton Research 9, 327–344.

Cullen, J.J., MacIntyre, J.G., 1998. Behavior, physiology and the niche of depth-regulating phytoplankton. In: Anderson, D.M., Cembella, A.D., Hallegraeff, G.M. (Eds.), Physiological Ecology of Harmful Algal Blooms. Springer, Berlin, pp. 559–579.

Depinto, J.V., Verhoff, F.H., 1977. Nutrient regeneration from aerobic decomposition of green-algae. Environmental Science & Technology 11, 371–377.

Diehl, S., 2002. Phytoplankton, light, and nutrients in a gradient of mixing depths: Theory. Ecology 83, 386–398.

Diehl, S., Berger, S., Ptacnik, R., Wild, A., 2002. Phytoplankton, light, and nutrients in a gradient of mixing depths: field experiments. Ecology 83, 399–411.

Du, Y., Hsu, S.-B., 2008. Concentration phenomena in a nonlocal quasi-linear problem modelling phytoplankton II: limiting profile. SIAM Journal on Mathematical Analysis 40, 1441–1470.

Fee, E.J., 1976. Vertical seasonal distribution of chlorophyll in lakes of Experimental-Lakes-Area, Northwestern Ontario implications for primary production estimates. Limnology & Oceanography 21, 767–783.

Fennel, K., Boss, E., 2003. Subsurface maxima of phytoplankton and chlorophyll: steady-state solutions from a simple model. Limnology & Oceanography 48, 1521–1534.

Field, C.B., Behrenfeld, M.J., Randerson, J.T., Falkowski, P., 1998. Primary production of the biosphere: integrating terrestrial and oceanic components. Science 281, 237–240.

Gonsiorczyk, T., Casper, P., Koschel, R., 1998. Phosphorus-binding forms in the sediment of an oligotrophic and an eutrophic hardwater lake of the Baltic lake district (Germany). Water Science & Technology 37, 51–58.

Gross, H.P., Wurtsbaugh, W.A., Luecke, C., Budy, P., 1997. Fertilization of an oligotrophic lake with a deep chlorophyll maximum: predicting the effect on primary productivity. Canadian Journal of Fisheries & Aquatic Sciences 54, 1177–1189.

Hartmann, J., Kunimatsu, T., Levy, J.K., 2008. The impact of Eurasian dust storms and anthropogenic emissions on atmospheric nutrient deposition rates in forested Japanese catchments and adjacent regional seas. Global & Planetary Change 61, 117–134.

Hays, G.C., Richardson, A.J., Robinson, C., 2005. Climate change and marine plankton. Trends in Ecology & Evolution 20, 337–344.

Hodges, B.A., Rudnick, D.L., 2004. Simple models of steady deep maxima in chlorophyll and biomass. Deep-Sea Research Part I—Oceanographic Research Papers 51, 999–1015.

Holopainen, A.L., Niinioja, R., Rämö, A., 2003. Seasonal succession, vertical distribution and long term variation of phytoplankton communities in two shallow forest lakes in eastern Finland. Hydrobiologia 506, 237–245.

Huisman, J., 1999. Population dynamics of light-limited phytoplankton: microcosm experiments. Ecology 80, 202–210.

Huisman, J., van Oostveen, P., Weissing, F.J., 1999. Critical depth and critical turbulence: two different mechanisms for the development of phytoplankton blooms. Limnology & Oceanography 44, 1781–1787.

Huisman, J., Sharples, J., Stroom, J.M., Visser, P.M., Kardinaal, W.E.A., Verspagen, J.M.H., Sommeijer, B., 2004. Changes in turbulent mixing shift competition for light between phytoplankton species. Ecology 85, 2960–2970.
Huisman, J., Sommeijer, B., 2002a. Maximal sustainable sinking velocity of phytoplankton. Marine Ecology—Progress Series 244, 39–48.
Huisman, J., Sommeijer, B., 2002b. Population dynamics of sinking phytoplankton in light-limited environments: simulation techniques and critical parameters. Journal of Sea Research 48, 83–96.
Huisman, J., Thi, N.N.P., Karl, D.M., Sommeijer, B., 2006. Reduced mixing generates oscillations and chaos in the oceanic deep chlorophyll maximum. Nature 439, 322–325.
Huisman, J., Weissing, F.J., 1994. Light-limited growth and competition for light in well-mixed aquatic environments: an elementary model. Ecology 75, 507–520.
Huisman, J., Weissing, F.J., 1995. Competition for nutrients and light in a mixed water column—a theoretical-analysis. American Naturalist 146, 536–564.
Hutchinson, G.E., 1957. A Treatise on Limnology. John Wiley & Sons.
Jäger, C.G., Diehl, S., Emans, M., 2010. Physical determinants of phytoplankton production, algal stoichiometry, and vertical nutrient fluxes. American Naturalist 175, E91–E104.
Jöhnk, K.D., Huisman, J., Sharples, J., Sommeijer, B., Visser, P.M., Stroom, J.M., 2008. Summer heatwaves promote blooms of harmful cyanobacteria. Global Change Biology 14, 495–512.
Karlsson, J., Byström, P., Ask, J., Ask, P., Persson, L., Jansson, M., 2009. Light limitation of nutrient-poor lake ecosystems. Nature 460, 506–509.
Kirk, J.T.O., 1975. Theoretical-analysis of contribution of algal cells to attenuation of light within natural-waters. 1. General treatment of suspensions of pigmented cells. New Phytologist 75, 11–20.
Klausmeier, C.A., Litchman, E., 2001. Algal games: the vertical distribution of phytoplankton in poorly mixed water columns. Limnology & Oceanography 46, 1998–2007.
Krause-Jensen, D., Sand-Jensen, K., 1998. Light attenuation and photosynthesis of aquatic plant communities. Limnology & Oceanography 43, 396–407.
Kunz, T.J., Diehl, S., 2003. Phytoplankton, light and nutrients along a gradient of mixing depth: a field test of producer-resource theory. Freshwater Biology 48, 1050–1063.
Lampert, W., McCauley, E., Manly, B.F.J., 2003. Trade-offs in the vertical distribution of zooplankton: ideal free distribution with costs? Proceedings of the Royal Society of London Series B—Biological Sciences 270 765–773.
Leibold, M.A., 1990. Resources and predators can affect the vertical distributions of zooplankton. Limnology & Oceanography 35, 938–944.
Lindholm, T., 1992. Ecological role of depth maxima of phytoplankton. Archiv für Hydrobiologie-Beiheft Ergebnisse der Limnologie 35, 33–45.
Lorenzen, M., Mitchell, R., 1973. Theoretical effects of artificial destratification on algal production in impoundments. Environmental Science & Technology 7, 939–944.
Lucas, L.V., Cloern, J.E., Koseff, J.R., Monismith, S.G., Thompson, J.K., 1998. Does the sverdrup critical depth model explain bloom dynamics in estuaries? Journal of Marine Research 56 375–415.
MacIntyre, S., Flynn, K.M., Jellison, R., Romero, J.R., 1999. Boundary mixing and nutrient fluxes in Mono Lake, California. Limnology & Oceanography 44, 512–529.
Magnuson, J.J., Webster, K.E., Assel, R.A., Bowser, C.J., Dillon, P.J., Eaton, J.G., Evans, H.E., Fee, E.J., Hall, R.I., Mortsch, L.R., Schindler, D.W., Quinn, F.H., 1997. Potential effects of climate changes on aquatic systems: laurentian great lakes and precambrian shield region. Hydrological Processes 11, 825–871.
Mann, K.H., Lazier, J.R.N., 1996. Dynamics of marine ecosystems: biological–physical interacting in the oceans. Blackwell Science.
Marsden, M.W., 1989. Lake restoration by reducing external phosphorus loading—the influence of sediment phosphorus release. Freshwater Biology 21, 139–162.
Mellard, J.P., 2010. The vertical distribution of phytoplankton: observations, theory, experiments. Ph.D. Thesis, Michigan State University.
Moll, R.A., Stoermer, E.F., 1982. A hypothesis relating trophic status and subsurface chlorophyll maxima of lakes. Archiv für Hydrobiologie 94, 425–440.
Monsi, M., Saeki, T., 1953. On the factor light in plant communities and its importance for matter production. Japanese Journal of Botany 14, 22–52.
Neff, J.C., Ballantyne, A.P., Farmer, G.L., Mahowald, N.M., Conroy, J.L., Landry, C.C., Overpeck, J.T., Painter, T.H., Lawrence, C.R., Reynolds, R.L., 2008. Increasing eolian dust deposition in the western United States linked to human activity. Nature Geoscience 1, 189–195.
Okubo, A., 1980. Diffusion and Ecological Problems: Mathematical Models. Springer-Verlag.
O'Reilly, C.M., Alin, S.R., Plisnier, P.D., Cohen, A.S., McKee, B.A., 2003. Climate change decreases aquatic ecosystem productivity of Lake Tanganyika, Africa. Nature 424, 766–768.
Osborn, T.R., 1980. Estimates of the local-rate of vertical diffusion from dissipation measurements. Journal of Physical Oceanography 10, 83–89.
Paerl, H.W., 1988. Nuisance phytoplankton blooms in coastal, estuarine, and inland waters. Limnology & Oceanography 33, 823–847.
Paerl, H.W., Huisman, J., 2009. Climate change: a catalyst for global expansion of harmful cyanobacterial blooms. Environmental Microbiology Reports 1, 27–37. Limnology & Oceanography 18, 821–839.
Peeters, F., Straile, D., Lorke, A., Ollinger, D., 2007. Turbulent mixing and phytoplankton spring bloom development in a deep lake. Limnology & Oceanography 52, 286–298.
Peters, R.H., Rigler, F.H., 1973. Phosphorus release by Daphnia. Limnology & Oceanography 18, 821–839.
Portielje, R., Lijklema, L., 1999. Estimation of sediment-water exchange of solutes in Lake Veluwe, the Netherlands. Water Research 33, 279–285.
Reynolds, C.S., 1984. The Ecology of Freshwater Phytoplankton. Cambridge University Press.
Ross, O.N., Sharples, J., 2007. Phytoplankton motility and the competition for nutrients in the thermocline. Marine Ecology—Progress Series 347, 21–38.
Ryabov, A.B., Rudolf, L., Blasius, B., 2010. Vertical distribution and composition of phytoplankton under the influence of an upper mixed layer. Journal of Theoretical Biology 263, 120–133.
Sand-Jensen, K., Borum, J., 1991. Interactions among phytoplankton, periphyton, and macrophytes in temperate freshwaters and estuaries. Aquatic Botany 41, 137–175.
Schindler, D.W., 1997. Widespread effects of climatic warming on freshwater ecosystems in North America. Hydrological Processes 11, 1043–1067.
Sharpley, A., Daniel, T.C., Sims, J.T., Pote, D.H., 1996. Determining environmentally sound soil phosphorus levels. Journal of Soil & Water Conservation 51, 160–166.
Steele, J.H., 1978. Some comments on plankton patches. Spatial pattern in plankton communities. NATO Conference Series IV: Marine Sciences, vol. 3. Plenum Press, New York, pp. 1–20.
Tilman, D., 1982. Resource Competition and Community Structure. Princeton University Press, Princeton NJ.
Verburg, P., Hecky, R.E., Kling, H., 2003. Ecological consequences of a century of warming in Lake Tanganyika. Science 301, 505–507.
Visser, P.M., Ibelings, B.W., vanderVeer, B., Koedood, J., Mur, L.R., 1996. Artificial mixing prevents nuisance blooms of the cyanobacterium Microcystis in Lake Nieuwe Meer, the Netherlands. Freshwater Biology 36, 435–450.
Waite, A., Fisher, A., Thompson, P.A., Harrison, P.J., 1997. Sinking rate versus cell volume relationships illuminate sinking rate control mechanisms in marine diatoms. Marine Ecology—Progress Series 157, 97–108.
Walsby, A.E., 1994. Gas vesicles. Microbiological Reviews 58, 94–144.
Walsby, A.E., Hayes, P.K., Boje, R., Stal, L.J., 1997. The selective advantage of buoyancy provided by gas vesicles for planktonic cyanobacteria in the Baltic Sea. New Phytologist 136, 407–417.
Wetzel, R.G., 1975. Limnology. W.B. Saunders Company.
Williamson, C.E., Sanders, R.W., Moeller, R.E., Stutzman, P.L., 1996. Utilization of subsurface food resources for zooplankton reproduction: implications for diel vertical migration theory. Limnology & Oceanography 41, 224–233.
Wüest, A., Piepke, G., Van Senden, D.C., 2000. Turbulent kinetic energy balance as a tool for estimating vertical diffusivity in wind-forced stratified waters. Limnology & Oceanography 45, 1388–1400.
Yoshiyama, K., Mellard, J.P., Litchman, E., Klausmeier, C.A., 2009. Phytoplankton competition for nutrients and light in a stratified water column. American Naturalist 174, 190–203.
Yoshiyama, K., Nakajima, H., 2002. Catastrophic transition in vertical distributions of phytoplankton: alternative equilibria in a water column. Journal of Theoretical Biology 216, 397–408.